Slide-away distributions and relevant collective modes in high-temperature plasmas

NUCLEAR FUSION 16 2 (1976)

SLIDE-AWAY DISTRIBUTIONS AND RELEVANT COLLECTIVE MODES IN HIGH-TEMPERATURE PLASMAS

B. COPPI, F. PEGORARO*, R. POZZOLI**, G. REWOLDT***
Massachusetts Institute of Technology,
Cambridge, Massachusetts,
United States of America

ABSTRACT. The evolution of the electron distribution function, when an electric field that is not too small in comparison with the critical electron runaway field is applied along the confining magnetic field of a high temperature plasma, is analysed. In the regimes considered, a finite fraction of the electron population has magnetically trapped orbits, and is not appreciably affected by the applied electric field, while the distribution of circulating electrons tends to "slide away" as a whole. Then the Spitzer-Härm model for the current-carrying electron distribution is inadequate, and the role that collective modes, in particular current-driven microinstabilities, and collisions can play in producing a stationary electron distribution is analysed. Modes at the ion plasma frequency, ω_{pi}, that are driven by the positive slope of the current-carrying electron distribution, can be excited, when the average electron drift velocity is a finite fraction of the electron thermal velocity, and transfer transverse energy to the main body of the electron distribution. These features are consistent with the experimental observations performed on the Alcator device. Modes at the "reduced" electron plasma frequency $(k_{\parallel}/k)\omega_{pe}$ can also be excited both in connection with the modes at ω_{pi} and independently. Modes at the electron gyrofrequency Ω_e associated with the loss-cone feature that the electron distribution tends to develop are considered, among others, as a factor for the strongly enhanced electron cyclotron emission experimentally observed in regimes where non-thermal electron distributions have been realized.

1. INTRODUCTION

In the present paper, we deal with the problem of the evolution of the electron distribution function when an electric field that is not too small in comparison with the critical electron runaway field is applied along the confining magnetic field of a high-temperature plasma. In particular, we consider regimes in toroidal configurations where a finite fraction of the electron population has magnetically trapped orbits. Therefore, over time scales larger than their average bounce time, trapped electrons are not appreciably affected by the applied electric field, while the distribution of circulating electrons tends to "slide away" as a whole if the electric field is a finite fraction of the critical runaway field. In these conditions, the Spitzer-Härm [1] model for the current-carrying electron distribution is not adequate [2], and we analyse the role that collective modes, in particular current-driven microinstabilities, and collisions can have in producing a stationary electron distribution.

In Section 2, we analyse the evolution of the electron distribution function in the absence of collisions, by the Vlasov equation. For this, the particle orbits are studied in an axisymmetric toroidal magnetic confinement configuration with an externally induced electric field $\vec{E}_{\parallel}$.

The single-particle analysis is then used to integrate numerically the Vlasov equation in the drift approximation. A markedly non-Maxwellian distribution function is thereby obtained. We notice that this distribution tends to develop a 'loss-cone' in the direction contrary to that of acceleration and an interval of positive slope in the direction of acceleration.

In Section 3, the topological and physical properties of the modes that can develop in an axisymmetric toroidal configuration are investigated [3], with special reference to the effects of magnetic shear [4] and to the question of localization in the poloidal direction [5].

In Section 4, modes with frequencies between the ion and the electron cyclotron frequencies are examined. It is shown that a distribution of the type derived in Section 2 (or, more generally, a distribution where a considerable portion is sliding away) can excite modes with frequencies around the ion plasma frequency ω_{pi}, which can resonate with the main body of the ion distribution and provide effective heating of it. This process is, in fact, proposed to explain the dramatic increase of the ion temperature which has been observed in the Alcator device [6], as the ratio of the electron drift velocity to the thermal velocity is raised above a given critical value that is a finite fraction. The spectrum of the relevant modes ranges from frequencies $\omega \simeq \omega_{pi}$ to $\omega \simeq (k_{\parallel}/k)\omega_{pe}$, where k is the mode wave-number and $k_{\parallel}$ is its component along the magnetic field. Another possible source of modes with frequency $(k_{\parallel}/k)\omega_{pe}$ is the temperature anisotropy of a long tail in the electron distribution. However, we find that the Landau damping from the main body of the distribution can easily overcome the growth rate of this instability, unless we assume that the main body of the electron distribution, approaching

* Permanent address: Istituto di Fisica, Università di Pisa, 65100 Pisa, Italy.
** Present address: Laboratorio di Fisica del Plasma, CNR, Milano, Italy.
*** Present address: Princeton University, Plasma Physics Laboratory, Princeton, New Jersey, USA.

the slide-away regime, develops a region of less steep slope than the one of a Maxwellian.

In Section 5, electron loss-cone modes at the harmonics of the electron cyclotron frequency are discussed. These modes are de-stabilized by the discontinuity of the electron distribution function at the boundary between the trapped- and the untrapped-particle regions. These modes are considered for an explanation of the strongly enhanced electron cyclotron emission, well above the thermal level, detected on Alcator [6] and possibly in other types of plasmas [7].

In Section 6, the main characteristics of modes with frequency $\omega \lesssim \Omega_i$ are briefly indicated. In particular, we recall from Ref.[8] that the ion cyclotron modes tend to be localized at the outside of the torus and to be damped whenever an appreciable fraction of the electron population is trapped. Then we argue that modes at the ion cyclotron frequency should not be suitable to explain the increase of the ion temperature which is observed in the slide-away regime. Finally, we point out that standing modes with frequency higher than or of the order of the electron transit frequency can transfer parallel momentum from the circulating to the trapped electrons, and then to the periodic inhomogeneous magnetic field, thereby producing anomalous resistivity [3, 9].

In Section 7, the relationships with experimental observations in Alcator are discussed. On the basis of the observed excitation of high-frequency fluctuations, and of the dependence of the average ratio of the observed electrical resistivity to the classical resistivity on the ratio of the electron drift velocity to the electron thermal velocity, three regimes can be identified: (I) A "nearly-classical" regime, for relatively low electron drift velocities. Here the electrical resistivity is not a decreasing function of the streaming parameter ξ which is defined as the ratio of the electron drift velocity to the thermal velocity; (II) An "intermediate" regime where no excitation of high-frequency fluctuations is observed and the ratio of the longitudinal to the classical resistivity is a decreasing function of ξ; (III) A "slide-away" regime which occurs for the largest values of ξ, above a critical value ξ_c that depends on the ion mass, and where the excitation of fluctuations with frequency about equal to and higher than the ion plasma frequency is observed [10]. The onset of these fluctuations is correlated with the onset of a region of positive slope in the distribution function of the current-carrying electrons, according to the theoretical indications presented in the previous sections. Finally, it is pointed out that in the intermediate and slide-away regimes, where the current results from a relatively large deformation of the electron distribution, the form of the corresponding electrical resistivity depends on the form of the electron thermal energy balance equation, while in the case of classical resistivity, this is defined only by the momentum balance equation and depends only on the electron temperature.

2. COLLISIONLESS EVOLUTION OF THE ELECTRON DISTRIBUTION FUNCTION

We consider a high-temperature toroidal plasma in an axisymmetric confinement configuration, where a toroidal current is driven by an externally induced electric field $\vec{E}$, and magnetic trapping occurs for a considerable fraction of the electron population.

We analyse the effects of the electric field on the evolution of the equilibrium electron distribution function in the collisionless limit in order to obtain indications for realistic cases where the behaviour of the electron distribution tends to be considerably different from the neoclassical model [11,12,2]. In this context, "equilibrium evolution" means the non-turbulent evolution of the electron distribution with a time scale $\tau_{eq} \sim (T_e m_e)^{1/2}/(eE)$, where T_e is the initial electron temperature, $-e$ is the electron charge, and m_e is the electron mass.

i) SINGLE-PARTICLE ANALYSIS

We refer to a confinement configuration in which a and R_0 are the minor and major radii of the torus, ζ is the toroidal angle, θ the poloidal angle and the magnetic surfaces have concentric circular cross-sections with radius r. The magnetic field is represented by the following equations:

$$B_\zeta = B_0/h(r,\theta) \quad \text{and} \quad B_\theta = B_\zeta r/[R_0 q(r)] \tag{2.1}$$

where $h(r,\theta) = 1 + (r/R_0)\cos\theta$ and $q(r)$ is the inverse rationalized rotational transform. Then $|B_\theta/B_\zeta| \sim a/(R_0 q)$. The externally induced electric field $\vec{E}$ is assumed to be nearly constant in time and represented by

$$E_\zeta(r,\theta) \simeq E_0/h(r,\theta) \tag{2.2}$$

so that $\nabla \times \vec{E} \simeq 0$ inside the torus. In the guiding-centre approximation the particle drift velocity perpendicular to the magnetic field is

$$\vec{v}_\perp = \{(v_\parallel^2 + \mu B/m_e)(\vec{B}/B^3)\times\nabla(B^2/2) + (v_\parallel^2/B)(\nabla\times\vec{B})\}/\Omega + c\vec{E}\times\vec{B}/B^2 \tag{2.3}$$

where $\mu = m_e v_\perp^2/2B$ is the particle magnetic moment and $\Omega = -eB/m_e c$. The motion along the field lines is given by

$$m_e \frac{dv_\parallel}{dt} = -eE_\parallel - \mu \frac{\vec{B}\cdot\nabla(B^2/2)}{B^2} + m_e c v_\parallel (\vec{E}\times\vec{B}) \cdot \frac{\vec{B}\cdot\nabla(\vec{B}/B)}{B^3} \tag{2.4}$$

Referring to the electron orbits, it is convenient to introduce the following dimensionless quantities:

$$\rho \equiv r/a$$

$$\tau \equiv \frac{t}{q_0 R_0}\left(\frac{\mu B_0}{m_e}\frac{a}{R_0}\right)^{1/2}$$

$$\eta^2 \equiv \frac{m_e v_{\parallel}^2}{\mu B_0}\frac{R_0}{a} \qquad (2.5)$$

$$\alpha \equiv \frac{e E_0 R_0 q_0}{\mu B_0}\frac{R_0}{a}$$

$$\rho_b \equiv \left(\frac{m_e \mu B_0 R_0}{a}\right)^{1/2}\frac{q_0 c}{e B_0 a}$$

where $q_0 \equiv q(a)$, τ is the time variable normalized to the electron "bounce frequency", η^2 is a pitch angle variable which is of order one for trapped electrons, α is normalized to the energy that the electric field must supply to a trapped electron in order to untrap it, and ρ_b is the ratio of the radial excursion of a trapped electron to the minor radius a. Then, retaining only first-order terms in (a/R_0) and a term proportional to $(R_0 \rho_b / a\rho)$, Eqs (2.3) and (2.4) can be rewritten as

$$\frac{d(\rho/\rho_b)}{d\tau} \simeq \left[1 - \frac{a}{R_0}(\rho\cos\theta - \eta^2)\right]\sin\theta \qquad (2.6)$$

where the $\vec{E}\times\vec{B}$ term has been neglected,

$$\frac{d\theta}{d\tau} \simeq \left[\frac{\eta}{\hat{q}} + \frac{R_0\rho_b}{\rho a}\cos\theta\right] \qquad (2.7)$$

$$\frac{d\eta}{d\tau} \simeq -\left[\frac{\rho}{\hat{q}}\sin\theta + \alpha - \frac{a}{R_0}\rho\cos\theta\left(\frac{2\rho}{\hat{q}}\sin\theta + \alpha\right)\right] \qquad (2.8)$$

and $\hat{q}(\rho) \equiv q(\rho)/q_0$.

On the basis of these equations, we see that most of the trapped-electron population does not experience a net acceleration along the magnetic field lines and is driven inward with a radial drift velocity proportional to E_ζ / B_θ (Ware drift), while circulating electrons are accelerated and the relevant distribution slides away. This behaviour is easily shown by retaining only the leading-order terms in Eqs (2.6,7,8) and taking the time average over an orbit of the radial equation, i.e.

$$\left\langle \frac{d(\rho/\rho_b)}{d\tau}\right\rangle \simeq \langle \sin\theta\rangle + \frac{a}{R_0}\langle \eta^2 \sin\theta\rangle \qquad (2.9)$$

where the second term on the right-hand side must be considered only for circulating particles. The leading-order terms of Eqs (2.7,8) give

$$\frac{d\theta}{d\tau} = \eta/\hat{q} \qquad (2.10)$$

and

$$\frac{d\eta}{d\tau} = -\frac{\rho\sin\theta}{\hat{q}} - \alpha \qquad (2.11)$$

where ρ is taken to be constant. From Eq.(2.11), in the case of trapped electrons, i.e. assuming $\langle d\eta/d\tau\rangle \simeq 0$, we obtain

$$\langle \sin\theta\rangle = -\frac{\hat{q}}{\rho}\alpha \qquad (2.12)$$

which substituted into Eq.(2.9) gives

$$v_{Dr} = -cE_\zeta / B_\theta \qquad (2.13)$$

This is the so-called Ware drift.

Then, from Eqs (2.10) and (2.11), we obtain

$$\frac{d^2\theta}{d\tau^2} = -\rho\frac{\sin\theta}{\hat{q}^2} - \frac{\alpha}{\hat{q}} \qquad (2.14)$$

In the absence of the electric field ($\alpha = 0$), the orbits in phase space, as described by Eq.(2.14), present the well-known behaviour shown in Fig.1 (bottom). The central region corresponds to trapped orbits (closed lines) and separates two regions corresponding to circulating orbits with positive and negative parallel velocity (open lines). A circulating particle cannot reverse its motion unless collisions or collective interactions with the other particles are taken into account. So, a transition between the three mentioned regions in phase space can be made possible only by collisions or collective interactions.

When a relatively weak electric field is applied, the distortion of the trapped-particle region is small, while the phase space trajectories of circulating particles change their topology. Then a non-collisional transition from one region of circulating particles ($v_\parallel < 0$) to the other ($v_\parallel > 0$) is induced (see Fig.1 (top)). For the electric field not to alter the region of magnetic trapping appreciably, the condition $\bar{\alpha} < 1$ has to be verified where $\bar{\alpha} = \alpha(\mu B_0 / T_e)$. Notice that, in the trapped-electron regimes, $\bar{\alpha} < 1$ is implied by the condition $E_0 \lesssim E_R$ where $E_R \equiv (m_e/e)\nu_e v_{the}$ is the electron runaway field and ν_e is the electron collision frequency.

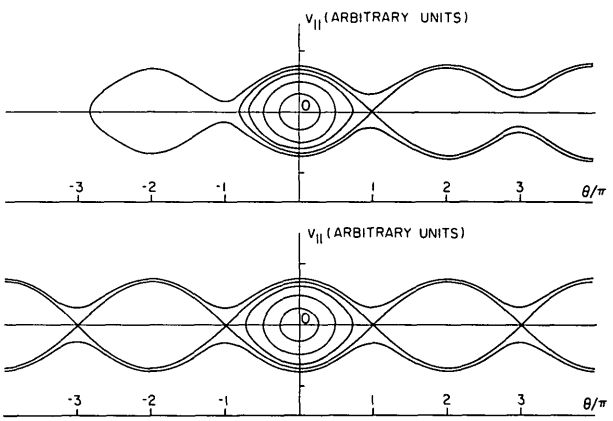

FIG. 1. (Top) Phase space trajectories relevant to Eq.(2.14) with $\bar{\alpha} \neq 0$. (Bottom) Phase space trajectories in the absence of the electric field ($\bar{\alpha} = 0$).

Following Eq.(2.14), the separatrix between the trapping and circulating region in velocity space is given by the following equation:

$$v_\perp = \left\{ \frac{R_0}{r(1+\cos\theta)} \left[v_\parallel^2 + \frac{2\alpha\mu B_0 a}{m_e R_0 q} (\theta+\pi) \right] \right\}^{1/2} \qquad (2.15)$$

ii) INCIPIENT BEHAVIOUR OF THE DISTRIBUTION FUNCTION

From the single-particle analysis previously presented, it is evident that, if neither collisions nor fluctuations were present, and if $\bar{\alpha} < 1$, the distribution function would show a separation between the trapped particles, which remain in the same region of velocity space, and the circulating particles, which are continuously accelerated by the electric field. The extent of this separation would be determined by collisional effects, and by wave-particle interactions driven by the strong non-equilibrium deformations of the distribution which will be considered in later sections.

The evolution of the electron distribution function in the absence of collisions has been computed by the direct use of the numerical solution of the equations of motion (2.6), (2.7), and (2.8). The initial distribution function is assumed to be Maxwellian and, for the sake of simplicity, uniform in space inside the torus:

$$f(t=0) \equiv f_0 = \exp(-v^2/v_{the}^2) \qquad (2.16)$$

where the normalization max(f) = 1 has been chosen.

The level curves of the initial distribution function are shown in Fig.2. The evolution of the electron distribution has been computed, with r fixed at the value $r/R_0 = 1/3.75$, at $\theta = 0$ and $\theta = \pi$. The level curves of the distribution functions at $\bar{\tau} = 25$ and $\bar{\tau} = 37.5$ are shown in Figs 3, 4, 5 and 6. Here $\bar{\tau} \equiv (T_e/\mu B_0)^{1/2}\tau$ and $T_e \simeq 1$ keV has been assumed. The following parameter values have been used, for the sake of illustration, in the numerical computations: $R_0 = 60$ cm, $a = 20$ cm, $q_0 = 3$, $\bar{\alpha} = 3\times10^{-2}$, $\bar{\rho}_b \equiv (T_e/\mu B_0)^{1/2}\rho_b = 3.7\times10^{-4}$.

It is intuitively clear that a distribution like that described in Figs 3 to 6 will be modified by the presence of collisions. In particular, a region of energy around the origin of Fig.2, such that

$$\nu_e \left(\frac{R_0}{r}\right)\left(\frac{T_e}{\epsilon}\right)^{3/2} > \left(\frac{2r}{R_0}\right)^{1/2}\left(\frac{\epsilon}{T_e}\right)^{1/2} \bar{\omega}_{te} \qquad (2.17)$$

corresponding to

$$\left(\frac{v}{v_{the}}\right) \leq \left[\frac{2\nu_e}{\bar{\omega}_{te}}\left(\frac{R_0}{2r}\right)^{3/2}\right]^{1/4} \qquad (2.18)$$

is collision-dominated. Here $\epsilon = m_e v^2/2$, ν_e is the average electron collision frequency for a Maxwellian distribution and $\bar{\omega}_{te} = v_{the}/(qR_0)$ is the

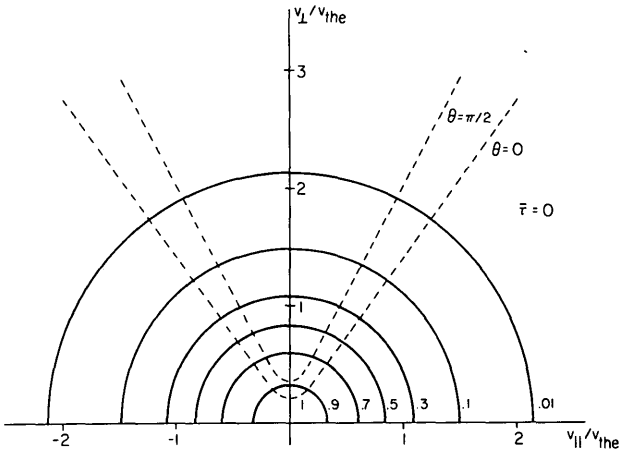

FIG. 2. Velocity space level curves of the initial (Maxwellian) electron distribution function. The maximum value of the distribution function has been normalized to one. The boundary between the trapped and circulating particle region is shown at $\theta = 0$ and $\theta = \pi/2$ for the parameters $R_0/a = 3$, $\rho = 0.8$, $\bar{\alpha} = 3 \times 10^{-2}$ and $q_0 = 3$.

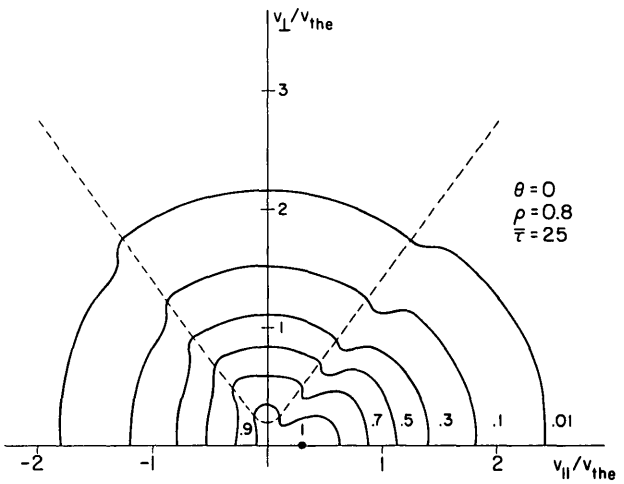

FIG. 3. Velocity space level curves of the electron distribution function at $\vartheta = 0$ and $\bar{\tau} = 25$.

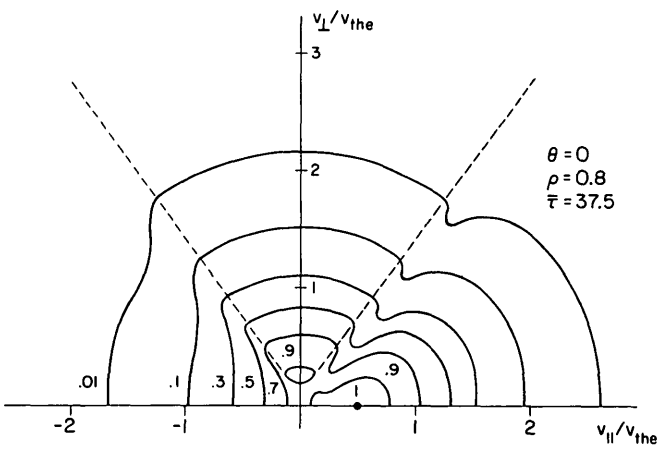

FIG. 4. Representation of the same level curves as in Fig.3, but at the time $\bar{\tau} = 37.5$.

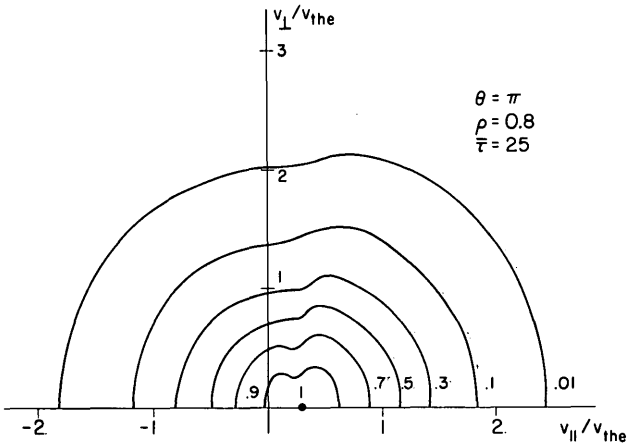

FIG. 5. Representation of the same level curves as in Fig. 3, but $\theta = \pi$ and $\bar{\tau} = 25$.

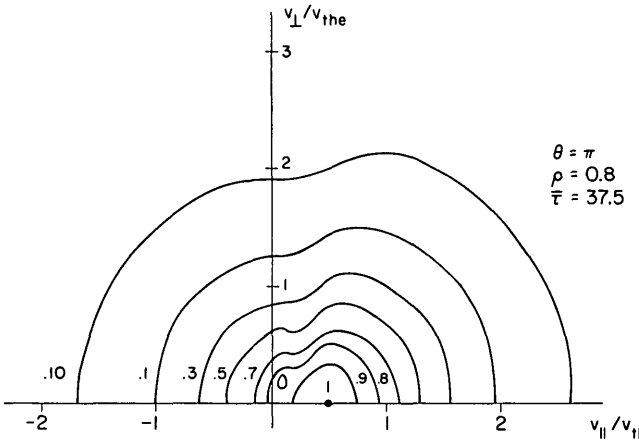

FIG. 6. Representation of the same level curves as in Fig. 3, but $\theta = \pi$ and $\bar{\tau} = 37.5$.

average transit frequency. In addition, wedge discontinuities, of the type appearing near the transition region between trapped and circulating electrons, can be filled in rather rapidly in terms of the average collision time ν_e^{-1}. On the other hand, if the applied electric field is a finite fraction of the runaway field E_R it is reasonable to assume that the distribution function will be distorted as indicated in Figs 3 to 6 for particle energies larger than thermal, and that collective modes such as those treated in Section 5 can fill in the produced "loss-cone" discontinuities.

3. TOROIDAL MODES

Referring to an axisymmetric toroidal confinement configuration in which ζ denotes the toroidal angle and θ the poloidal angle, as indicated earlier, the magnetic field can be represented by

$$\vec{B} = [B_0(r)\,\vec{e}_\zeta + B_\theta^0(r)\,\vec{e}_\theta]/(1+\epsilon_0\cos\theta) \tag{3.1}$$

Here $\epsilon_0 \equiv r/R_0$, R_0 is the toroidal major radius and r labels the relevant magnetic surfaces, which have been assumed to be concentric and of circular cross-section. We consider, for simplicity, the large-aspect-ratio limit where $\epsilon_0 \ll 1$ and $B_\theta^0 \ll B_0$. Then the inverse rationalized rotational transform of the magnetic field lines is given by

$$q(r) \equiv \frac{r\,B_\zeta}{R_0 B_\theta} \simeq \left.\frac{d\zeta}{d\theta}\right|_{\text{field line}} \tag{3.2}$$

The shear of the magnetic field is characterized by the dimensionless parameter

$$\hat{s}(r) = d\ln q/d\ln r = r\,q'/q \tag{3.3}$$

and we shall assume $\hat{s} \sim 1$, as a realistic limit.

We consider electrostatic modes for which the perturbed electric field $\tilde{\vec{E}} = -\nabla\tilde{\Phi}$, and we may write $\tilde{\Phi}$ in the form [3]

$$\tilde{\Phi} = \tilde{\phi}_{m^0,n^0}(\theta, r)\exp(-i\omega t + in^0\zeta - im^0\theta) \tag{3.4}$$

Here, $\tilde{\phi}_{m^0,n^0}$ is a periodic function in θ (slowly varying with respect to $\exp(-im^0\theta)$), not necessarily separable in r and θ, and m^0 and n^0 are integers. The perturbed electric field, parallel to the magnetic field, is

$$\tilde{E}_\parallel = -\frac{1}{B}\left(B_\theta\frac{1}{r}\frac{\partial\tilde{\Phi}}{\partial\theta} + B_\zeta\frac{1}{R}\frac{\partial\tilde{\Phi}}{\partial\zeta}\right)$$

$$= \frac{1}{R_0}\left[i\left(\frac{m^0}{q(r)} - n^0\right) - \frac{1}{q(r)}\left(\frac{\partial}{\partial\theta}\ln\tilde{\phi}_{m^0,n^0}\right)\right]\tilde{\Phi} \tag{3.5}$$

Correspondingly, the transverse perturbed electric field is

$$\tilde{\vec{E}}_\perp \approx \left[i\frac{m^0}{r}\vec{e}_\theta - \frac{1}{\tilde{\phi}_{m^0,n^0}}\frac{\partial\tilde{\phi}_{m^0,n^0}}{\partial r}\vec{e}_r\right]\tilde{\Phi} \tag{3.6}$$

From here on, we consider for simplicity only modes for which

$$\frac{m^0}{r} \gg \left|\frac{d\ln\tilde{\phi}_{m^0,n^0}}{dr}\right| \tag{3.7}$$

and $\tilde{E}_\perp \approx im^0\tilde{\Phi}/r$. For realistic current distributions inside the plasma column, q(r) is a monotonically increasing function of r, and $q(0) \leq q(r) \leq q(a)$, a being the radius of the plasma column. Then we distinguish modes for which

i) $q(a) < m^0/n^0$; or $m^0/n^0 < q(0)$ (3.8)

and

ii) $q(0) \leq m^0/n^0 \leq q(a)$ (3.9)

In the former case, we have

$$\tilde{E}_\parallel \approx \frac{i}{R_0}\left(\frac{m^0}{q(r)} - n^0\right)\tilde{\Phi} \tag{3.10}$$

and the relevant modes can be simulated by those typical of a one-dimensional plane geometry for which

$$\tilde{\Phi} = \tilde{\phi}(x) \exp(-i\omega t + ik_{\parallel} z + ik_{\perp} y) \tag{3.11}$$

with

$$k_{\parallel} = \frac{-1}{R_0}\left[\frac{m^0}{q(r)} - n^0\right] \quad \text{and} \quad k_{\perp} = -\frac{m^0}{r} \tag{3.12}$$

Then $|k_{\parallel}/k_{\perp}| \gtrsim r/[R_0 q(r)]$. In the following sections, we shall refer mostly to modes of this kind, that are current-driven and localized radially in the region where most of the plasma current is carried, such as around the maximum of $rJ_{\parallel}(r)$, $J_{\parallel}(r)$ being the longitudinal plasma current density. For the sake of simplicity, we shall consider $\tilde{\phi}_{m^0,n^0}$ constant, as a function of r, within an interval smaller than the region of its radial localization.

In the second case (ii), there exists a rational surface $r = r_0$ such that $m^0/n^0 = q(r = r_0) \equiv q_0$, and modes localized around this surface can be written as [3, 12]

$$\tilde{\Phi} = \tilde{\phi}_{m^0,n^0}(\theta, S) \exp\{-i\omega t + in^0[\zeta - q(r)\theta] + iS(r)\, F(\theta)\} \tag{3.13}$$

where $S(r) \equiv n^0[q(r) - q_0]$, $F(\theta)$ is a monotonic function of θ such that $F(\theta) = \int_0^{\theta} d\theta' G(\theta')$, $G(\theta)$ being periodic and even around $\theta = 0$, and $F(\theta + 2\pi) = F(\theta) + 2\pi$. Thus, $\tilde{\phi}_m(\theta) \equiv \tilde{\phi}_{m^0,n^0}(\theta, 0)$ represents the amplitude of a standing mode along a magnetic field line at $r = r_0$, the same mode being of the travelling type in the perpendicular direction. In this case,

$$\tilde{E}_{\parallel} = -\frac{\tilde{\Phi}}{qR_0}\frac{\partial}{\partial\theta}\ln\tilde{\phi}_{m^0,n^0} \tag{3.14}$$

on $r = r_0$, so that $|k_{\parallel}/k_{\perp}| < r/[R_0 q(r)]$, and, in a number of significant cases, $\tilde{\phi}_{m^0,n^0}(\theta, S)$ can be taken as periodic in S with period $\Delta S = 1$. We also notice that standing modes can be viewed as composed of pairs of waves with opposite phase velocities, and therefore have zero momentum along the magnetic field lines. In the case where $\tilde{\phi}_{m^0,n^0}(\theta, S) = \tilde{\phi}_{m^0,n^0}(\theta)$, we have flute modes on the rational surface $S = 0$ which are strongly affected by magnetic shear [4], and, therefore, we shall not devote special attention to this class of modes. In addition, we notice that, in high-temperature regimes where the particle collision mean free paths are much longer than $q(r)R_0$, the equilibrium distribution function may vary considerably as a function of θ because of the θ-variation in the fraction of trapped particles, and it is important to consider modes of either type i) or ii), localized in regions of θ, such as around $\theta = 0$ or $\theta = \pi$, where the fraction of trapped particles is maximum or minimum, respectively.

4. INSTABILITIES AROUND THE ION PLASMA FREQUENCY

A sequence of modes can be excited by particle-wave resonances in the region of positive slope of the electron distribution function that develops when (see Sections 2 and 7) a considerable fraction of the electron distribution function tends to slide away. In particular, we consider the frequency range $\Omega_i \ll \omega \ll |\Omega_e|$. In the description of the evolution of such a distribution, the modes in the lower-frequency part of this range, $\omega^2 \lesssim \omega_{pi}^2$, are of special importance since they can resonate both with the electron and the ion populations, and thus produce efficient anomalous momentum and energy transfer from the electrons to the ions. Since the modes in the frequency range under consideration have (parallel) wavelengths much shorter than the dimensions of the torus, they can be described in a linear geometry provided $k_{\parallel}/k \gtrsim \epsilon_0/q$ as shown in Section 3. They can thus be represented by

$$\tilde{\Phi} = \phi_k \exp(-i\omega t + ik_{\parallel} z + ik_{\perp} y) \tag{4.1}$$

where z is the direction along magnetic field lines. We look, in particular, for characteristics allowing these modes to resonate with the current-carrying part of the electron distribution and with the main body of the ion distribution at the same time. This is needed in order to produce effective ion heating while inducing longitudinal momentum transfer from the circulating electrons to the ions that restrains the relevant distribution from running away as a whole. Therefore, we consider modes for which the ions appear as unmagnetized and the electrons as magnetized, requiring, besides $\Omega_i \ll \omega \ll |\Omega_e|$, that

$$\frac{1}{\rho_i^2} \ll k_{\perp}^2 \ll \frac{1}{\rho_e^2} \tag{4.2}$$

The wave-particle resonance condition can be derived by a familiar quantum-mechanical model [13]. The relevant energy-momentum quantum numbers for the magnetized electrons are $v_{\parallel}$ and the magnetic quantum number N. For the ions, we can use the three components of the linear momentum. The energy and momentum conservation laws for the relevant wave-particle interactions are

$$\begin{aligned} \hbar\omega &= \hbar\Omega_e\, \Delta N + m_e v_{e\parallel}\, dv_{e\parallel} \\ \hbar k_{\parallel} &= m_e dv_{e\parallel} \\ \hbar\omega &= m_i \vec{v}_i \cdot d\vec{v}_i \\ \hbar\vec{k} &= m_i d\vec{v}_i \end{aligned} \tag{4.3}$$

and we consider the case $|\omega| \ll |\Omega_e|$ with $\Delta N = 0$. By substitution, the resonance condition becomes

$$\vec{k}\cdot\vec{v}_i = \omega = k_{\parallel} v_{e\parallel} \tag{4.4}$$

which is three-dimensional for the ions and only one-dimensional for the electrons. This indicates that longitudinal electron energy is transferred into mostly transverse energy of the resonating ions, for $k_\perp \gg k_\parallel$, while the transverse momentum acquired by the ions is taken up by the magnetic field. We also see that $m_i dv_{i\parallel} + m_e dv_{e\parallel} = 0$, and the longitudinal momentum transferred to the ions produces an effective resistivity. Notice that if we take $v_i \simeq v_{thi}$ and $v_{e\parallel} \sim v_{the}$ in the resonance condition, we have $k_\perp \sim k_\parallel (T_{e\parallel} m_i / T_i m_e)^{1/2} v_{the}$. From $\omega \simeq k v_i \simeq k_\perp v_{thi}$, we see that the conditions $\omega > \Omega_i$ and $k_\perp \rho_i > 1$ are equivalent. From $\omega \simeq k_\parallel v_{e\parallel} \simeq k_\parallel v_{the} \simeq k_\perp (T_i m_e / T_{e\parallel} m_i)^{1/2}$, we see that the condition $k_\perp \rho_e < 1$ implies $\omega < |\Omega_e|$.

With regard to the possible θ-localization of the modes under consideration, the most important θ-dependence in the dispersion relation should come from that of the electron distribution function in the slide-away regime. To avoid dealing with the complexity of the relevant dispersion relation that involves the operator $k_\parallel \simeq -(i/qR_0)\partial/\partial\theta$, we analyse two different models for the electron distribution function. In particular, we consider:

a) two Maxwellian distributions that are representative of the distribution around $\theta = 0$
b) one displaced Maxwellian distribution, that models the distribution without trapped electrons that occurs around $\theta = \pi$.

We find that the most unstable part of the spectrum has similar features in both cases. The frequency of this portion of the spectrum is $\omega^2 \lesssim \omega_{pi}^2$, and the quantity $u_e / v_{the} = -J/(env_{the})$, where J is the current density, is sufficient to describe the onset of the relevant instabilities and can be used to parametrize the sequence of modes that can be excited when u_e / v_{the} is increased (beyond a critical value of order $(2\epsilon_0)^{1/2}$ in case a)).

a) TWO-MAXWELLIAN MODEL FOR THE ELECTRON DISTRIBUTION

We notice that only the electron distribution integrated over $v_\perp$ is of interest in the case under consideration, where $|\omega| < |\Omega_e|$ and $b_e = (1/2)k_\perp^2 \rho_e^2 < 1$. The result of the integration over $v_\perp$ of the model slide-away distribution which will be given in Section 5 (see Eq.(5.2)), and which is shown in Fig.7, can be approximated near $\theta = 0$, at least qualitatively, by the sum of two Maxwellians

$$F_e \simeq n_0 (2\pi T_{e0}/m_e)^{-1/2} \exp\{-(v_\parallel / v_{the0})^2\} + n_1 (2\pi T_{e1}/m_e)^{-1/2} \exp\{-[(v_\parallel - u_1)/v_{the1}]^2\} \qquad (4.5)$$

where $T_{e0} = 2\epsilon_0 T_{e1}$ so that $v_{the0} = (2\epsilon_0)^{1/2} v_{the1}$, and $n_0 = n(2\epsilon_0)^{1/2}$ and $n_1 = n - n_0$. The parameter u_1 which gives the displacement of the second Maxwellian is related to u_e by

$$u_e = -J/n_e e = n_1 u_1 / n \qquad (4.6)$$

We represent the ion distribution by a single Maxwellian f_i with temperature $T_i = (1/\Theta) T_{el}$, so that $\Theta \geq 1$ for realistic parameters.

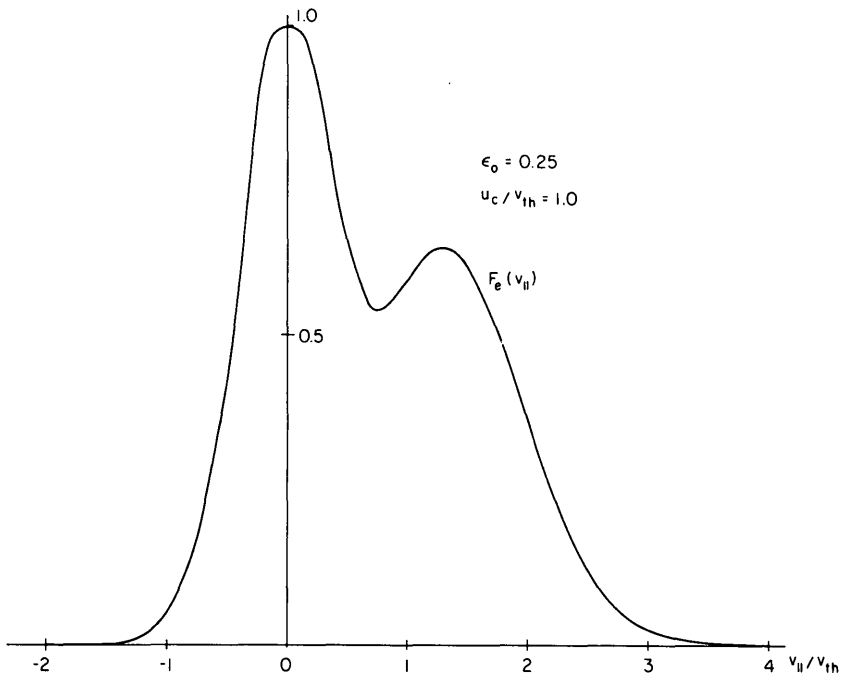

FIG. 7. Longitudinal electron distribution function $F_e(v_\parallel) \equiv \int d^2 v_\perp f_e(v_\parallel, v_\perp)$ obtained from the distribution function given by Eq. (5.2) which models the results obtained in Section 2. Here u_c is the parallel velocity of a circulating particle which, at $\tau = 0$, had $v_\parallel = v_\perp = 0$. Moreover, $u_c \simeq u_1$, where u_1 is the mean drift velocity of circulating electrons defined by Eq. (4.5).

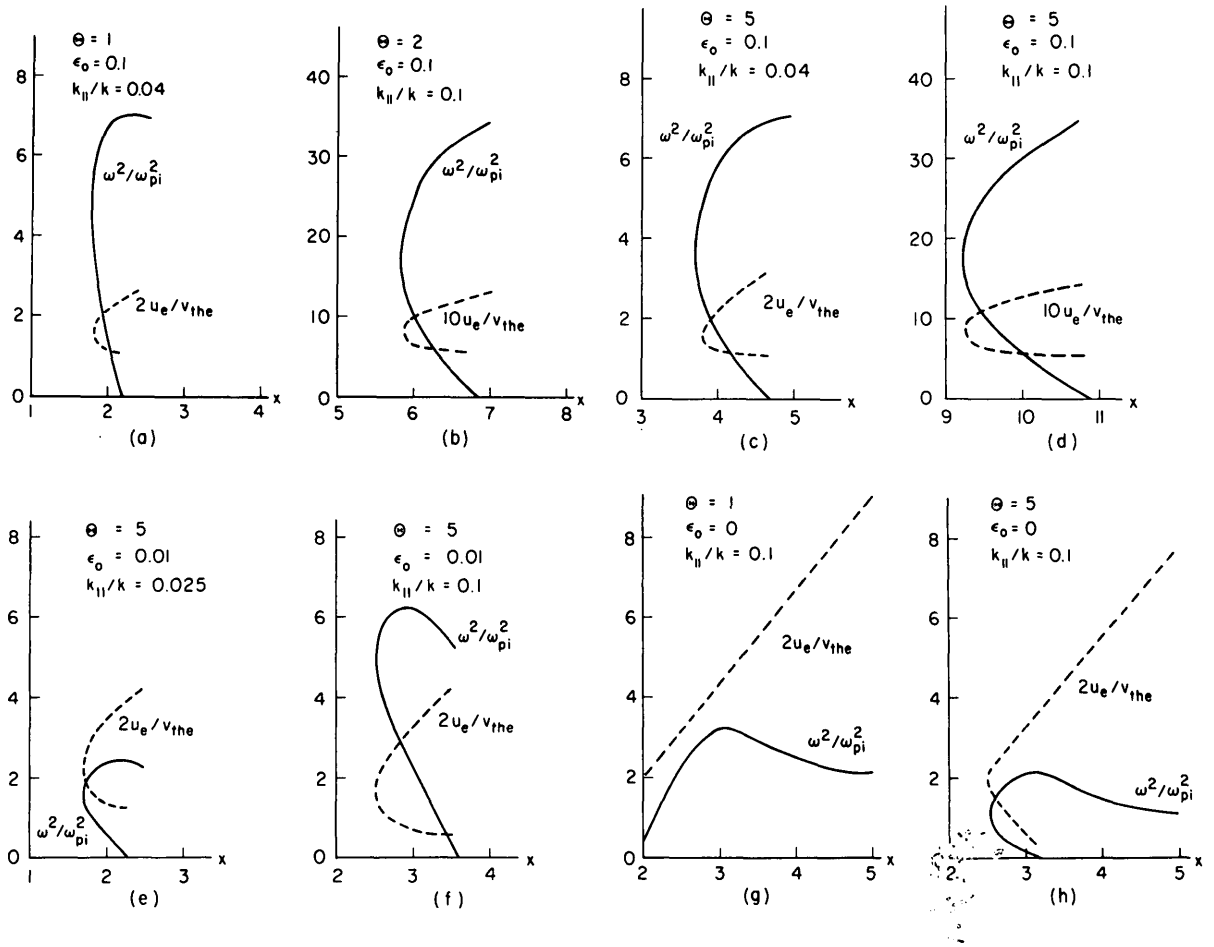

FIG. 8. Values of the dimensionless quantities ω^2/ω_{pi}^2 and u_e/v_{the} as functions of $x \equiv \omega/(k v_{thi})$ for different values of the parameters $\Theta \equiv T_{e1}/T_i$, ϵ_0 and $k_\parallel/k$, obtained by solving Eq. (4.3). The points on the upper part of each solid curve (ω^2/ω_{pi}^2) correspond to the points on the upper part of each dashed curve (u_e/v_{the}), and likewise for the lower parts.

The dispersion relation can be easily derived from the perturbed Vlasov equation for the ions

$$-i\omega \tilde{f}_i + i(\vec{k}\cdot\vec{v})\tilde{f}_i + \frac{e}{m_i}\tilde{\vec{E}}\cdot\nabla_v f_i^0 = 0 \qquad (4.7)$$

and

$$-i\omega\tilde{F}_e + i(k_\parallel v_\parallel)\tilde{F}_e - \frac{e}{m_e}\tilde{E}_\parallel \nabla_{v\parallel}\tilde{F}_e^0 = 0 \qquad (4.8)$$

for the electrons, by treating their distributions as one-dimensional along $\vec{B}$. Writing Poisson's equation and performing standard integrals we have [14]

$$\epsilon = 1 - \frac{1}{k^2\lambda_{Di}^2}\left\{W\left(\frac{\omega}{kv_{thi}}\right) + \frac{1}{\Theta}\left[\frac{n_1}{n}W\left(\frac{\omega - k_\parallel u_1}{k_\parallel v_{the1}}\right) + \frac{n_0 T_{e1}}{n T_{e0}}W\left(\frac{\omega}{k_\parallel v_{the0}}\right)\right]\right\} = 0 \qquad (4.9)$$

where ϵ is the dielectric constant,

$$W(x) = -(\pi)^{-1/2}\int_{-\infty}^{+\infty} d\xi \frac{\xi e^{-\xi^2}}{\xi - x} \qquad (4.10)$$

and $\lambda_{Di} \equiv (T_i/4\pi n e^2)^{1/2}$ is the ion Debye length.

To make a comparison with the experimental observations discussed in Section 7, we consider Eq. (4.9), in the limit where $\mathrm{Im}\,\omega = 0$, as representing a state of marginal stability that models the one obtained after a non-linear saturation process of the relevant instabilities has taken place. Equation (4.9) has, as a function of $x \equiv \omega/(kv_{thi})$, two branches of undamped solutions as shown in Fig. 8(a)-(f), where numerical results relative to the marginal stability condition of Eq. (4.9) have been plotted for different values of Θ, ϵ_0 and $k_\parallel/k$. Note that decreasing the value of $\epsilon_0 \equiv r/R_0$ corresponds to varying the radial position of the mode in the torus. In particular, a magnetic surface of special interest is the one on which $rJ(r)$ is maximum and, for the profile of $J(r)$ inferred for the Alcator experiment discussed in Section 7, this surface is close to $\epsilon_0 \approx 1/16$.

Then we may rewrite the real part of Eq.(4.9) as

$$\frac{\omega^2}{\omega_{pi}^2} = 2x^2 \mathrm{Re}\left\{ W(x) + \frac{1-(2\epsilon_0)^{1/2}}{\Theta} W[y(\Theta,x)] + \frac{(2\epsilon_0)^{1/2}}{\Theta} W\left[\frac{k}{k_\parallel} \left(\frac{m_e}{2m_i\epsilon_0\Theta} \right)^{1/2} x \right] \right\} \quad (4.11)$$

where $x = \omega/k v_{thi}$, $y = (\omega - k_\parallel u_1)/(k_\parallel v_{the1})$ is expressed as a function of x and Θ through the marginal stability condition,

$$\mathrm{Im}\, W_i + \frac{n_0 T_i}{n T_{e0}} \mathrm{Im}\, W_{e0} + \frac{n_1 T_i}{n T_{e1}} \mathrm{Im}\, W_{e1} = 0 \quad (4.12)$$

and the subscript to each W function indicates the population to which it refers. The lower branch of the two solutions of Eq.(4.11) corresponds to $\mathrm{Re}W_{e1} < 0$ and $\mathrm{Re}W_{e0} > 0$, such as in the case where

$$v_{the0} < \frac{\omega}{k_\parallel} ; \quad \left| \frac{\omega}{k_\parallel} - u_1 \right| < v_{the1}$$

Therefore, this can be considered to be like a "lower hybrid frequency mode" in relation to the trapped electrons, and like an "ion-sound mode" in relation to the circulating electrons. The ion term plays a dominant role in determining ω from Eq.(4.11).

Along the upper branch, however, the two electron contributions have the same sign ($\mathrm{Re}\, W_{e1} \gtrsim 0$), so that the frequency is approximately $\omega^2 \simeq (k_\parallel/k)^2 \omega_{pe}^2\, n_0/n$, where n_0 is roughly the number density of trapped particles. This is sometimes referred to as the Gould-Trivelpiece mode. We also recall that $\omega_{pi}/\Omega_i = 43.2\, \hat{n}^{1/2}/\hat{B}$, where $\hat{n} \equiv n/(10^{13}\ \mathrm{cm}^{-3})$ and $\hat{B} \equiv B/(10\ \mathrm{kG})$. As is shown in Figs 8(a) - (f), the solution of the dispersion relation (4.11) depends rather strongly on the actual values of Θ, ϵ_0 and $k_\parallel/k$. We may notice in addition the following qualitative features:

i) The resonant velocity $\omega/k_\parallel$ is near the minimum inside the electron distribution function.

ii) The threshold value of $\hat{u}_e \equiv u_e/v_{the}$, increases clockwise along the curves for $\omega^2/\omega_{pi}^2 = \hat{\omega}^2(x)/\omega_{pi}^2$.

iii) The lower branch is the most unstable part of the spectrum since the growth rate γ is an increasing function of $\Delta\hat{u} = \hat{u}_e - \hat{u}_{ethr}$. Thus the amplitude spectrum should be peaked in the most unstable region, i.e. $\omega^2 \lesssim \omega_{pi}^2$.

iv) The threshold value of $\hat{u}_e$ along the lower branch decreases as ϵ_0 decreases [15], increases with $k/k_\parallel$ and decreases with Θ (the actual slope depends on $k_\parallel/k$ and ϵ_0).

v) The phase velocity ω/k along the lower branch increases with Θ and decreases with ϵ_0 and $k/k_\parallel$. The quantity $\omega/(k v_{thi})$ measures the strength of the resonance of the mode with the ions.

b) DISPLACED ONE-MAXWELLIAN DISTRIBUTION

In this case we assume that the electron longitudinal distribution function can be approximated by a single Maxwellian centred at $v_\parallel = u_1 \equiv u_e$.

Thus the dispersion relation is

$$\epsilon = 1 - \frac{1}{k^2\lambda_{Di}^2} \left\{ W\left(\frac{\omega}{k v_{thi}} \right) + \frac{1}{\Theta} W\left(\frac{\omega - k_\parallel u_1}{k_\parallel v_{the}} \right) \right\} = 0 \quad (4.13)$$

If $\Theta = 1$, the condition of marginal stability is given by

$$\omega/(k v_{thi}) = -(\omega - k_\parallel u_1)/(k_\parallel v_{the}) \quad (4.14)$$

so that the wave is destabilized by the electrons and damped by the ions. The real part of the dispersion relation is then

$$\frac{\omega^2}{\omega_{pi}^2} = 4 \frac{\omega^2}{k^2 v_{thi}^2} W\left(\frac{\omega}{k v_{thi}} \right) \quad (4.15)$$

which is plotted in Fig.8(g). The instability threshold is $u_e/v_{the} \gtrsim 1$.

In the more interesting case $\Theta > 1$, Eq.(4.15) has, similar to case a), two branches of undamped solutions, which are plotted in Fig.8(h) for $\Theta = 5$ and $k_\parallel/k = 1/10$:

i) along the lower branch $|(\omega - k_\parallel u_1)/k_\parallel v_{the}|$ is less than one, so that $W_e \gtrsim -1$, the phase velocity ω/k is larger than v_{thi} so that $W_i \simeq (1/2)k^2 v_{thi}^2/\omega^2$, and ω^2/ω_{pi}^2 ranges from $k^2\lambda_{De}^2/(1+k^2\lambda_{De}^2)$ to 1. The threshold value of u_e/v_{the} increases with the frequency, from say 0.5 to 1, and decreases with Θ ($\hat{u}_e \simeq 0.4$ at $\Theta \simeq 10$);

ii) along the upper branch, $\omega/k v_{thi}$ and $-(\omega - k_\parallel u_1)/k v_{the}$ are almost equal and larger than one, $\omega^2 \simeq \omega_{pi}^2$, and the threshold value of u_e/v_{the} is an increasing function of the phase velocity. Since γ is an increasing function of $\Delta u_e \equiv u_e - u_{ethr}$, the lower branch is the most unstable part of the spectrum. A distinctive property of case a) compared to case b) is given by the limit of the threshold value of u_e/v_{the} for Θ large, which is finite in the two-Maxwellian approximation, due to the presence of the trapped particles, and goes to zero when the electron distribution function is approximated by a single displaced Maxwellian.

c) QUASI-LINEAR ESTIMATES

The time evolution of the average distribution functions $F_e^0(v_\parallel)$ and $f_i^0(\vec{v})$ under the action of the modes described in this section can be estimated from the quasi-linear diffusion equations [16,17]

$$\frac{\partial f_i^0}{\partial t} \simeq i \frac{e^2}{m_i^2} \sum_{\vec{k}} \frac{|E_{\vec{k}}|^2}{k^2} \vec{k} \cdot \frac{\partial}{\partial \vec{v}} \frac{1}{\omega - \vec{k}\cdot\vec{v}} \vec{k} \cdot \frac{\partial}{\partial \vec{v}} f_i^0 \quad (4.16)$$

and

$$\frac{\partial F_e^0}{\partial t} - \frac{e}{m_e} E_0 \frac{\partial F_e^0}{\partial v_\parallel} \simeq i \frac{e^2}{m_e^2} \sum_{\vec{k}} \frac{|E_{\vec{k}}|^2}{k^2} k_\parallel \frac{\partial}{\partial v_\parallel} \times \frac{1}{\omega - k_\parallel v_\parallel} k_\parallel \frac{\partial}{\partial v_\parallel} F_e^0 \quad (4.17)$$

where $E = E_0 \vec{e}_z$ is the external electric field, f_i^0 is the unperturbed ion distribution, F_i^0 is the unperturbed electron distribution integrated over $v_\perp$, and the summations extend over the wavelength spectrum. The relevant moments of Eqs (4.16) and (4.17) are

$$\frac{\partial}{\partial t}\vec{P}_i \simeq -\sum_{\vec{k}} \left|\frac{e\phi_{\vec{k}}}{T_i}\right|^2 \vec{k}\, T_i\, \mathrm{Im}\, W_i \qquad (4.18)$$

$$\frac{\partial}{\partial t} P_{e\parallel} + eE_0 \simeq -\sum_{\vec{k}} \left|\frac{e\phi_{\vec{k}}}{T_{e1}}\right|^2 k_\parallel T_{e1} \left[\frac{n_1}{n}\mathrm{Im}\, W_{e1} + \frac{n_0}{n}\frac{T_{e1}}{T_{e0}}\mathrm{Im}\, W_{e0}\right] \qquad (4.19)$$

$$\frac{\partial}{\partial t}\mathscr{E}_{i_\perp}\Big|_{turb} \approx \frac{\partial \mathscr{E}_i}{\partial t}\Big|_{turb} = -\frac{\partial \mathscr{E}_{e\parallel}}{\partial t}\Big|_{turb} = -\left|\frac{\omega}{k_\parallel}\right|\frac{\partial P_{e\parallel}}{\partial t}\Big|_{turb} \qquad (4.20)$$

where $\vec{P}_i = (m_i/n)\int d^3v\, \vec{v} f_i^0$, $P_{e\parallel} = (m_e/n)\int dv_\parallel v_\parallel F_e^0$, $\mathscr{E}_{i\perp} = (m_i/2n)\int d^3v\, v_\perp^2 f_i^0$, $\mathscr{E}_i = (m_i/2n)\int d^3v\, v^2 f_i^0$, $\mathscr{E}_{e\parallel} = (m_e/2n)\int dv_\parallel v_\parallel^2 F_e^0$, and the subscript "turb" means "due to the effect of the instability". Notice that, since for the electrons $|\Omega_e| > |\omega|$, the transverse momentum balance conservation is not considered.

The solutions of Eqs (4.16) to (4.20) depend critically on the phase velocity of the mode with respect to the ion distribution. If $\omega/(k v_{thi})$ is moderately larger than one, so that $\mathrm{Im}\, W_i$ is not too small, Eqs (4.18) and (4.20) indicate that a significant transfer of momentum to the ions and ion heating can be produced. This mechanism gives an effective rate of longitudinal momentum loss that we define by $m_e \nu_{turb} \cdot n u_e = \partial P_{i\parallel}/\partial t$, and is given by

$$\nu_{turb} = -\sum_{\vec{k}} \frac{4\pi k_\parallel}{m_e u_e}\left|\frac{e\phi_{\vec{k}}}{T_i}\right|^2 T_i\, \mathrm{Im}\, W_i \qquad (4.21)$$

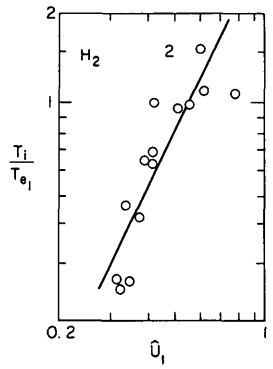

FIG. 9. Logarithmic diagram of the ratio of the ion temperature T_i to the electron temperature T_{e1} versus u_1/v_{the} in the slide away regime, after Ref. [18]. The parabolic-law fit of the data is shown by the solid line.

Note that when an electric field which is a finite fraction of the collisional runaway field (as it is in our case) is applied, the resistivity should, classically, go to zero since collisions are no longer sufficient to absorb the momentum of the electrons. The resistivity which is found under these conditions, for example, the one measured on Alcator (see Section 7), is thus "infinitely" anomalous, and is made up of non-collisional contributions of the type described by Eq.(4.21). Evidently, if $\omega/(k v_{thi})$ is considerably larger than unity, there is no resonant transfer of momentum and energy to the ions. For $u_e > u_{ethr}$, so that $\gamma > 0$, we can separate the resonant and the non-resonant quasi-linear diffusion of the electrons in Eq.(4.17), which gives

$$\frac{\partial F_e^0}{\partial t} - \frac{e}{m_e}E_0\frac{\partial F_e^0}{\partial v_\parallel} = \frac{e^2}{m_e^2}\sum_{\vec{k}}\frac{|E_{\vec{k}}|^2}{k^2}k_\parallel\frac{\partial}{\partial v_\parallel}\left[\pi\delta(\omega - k_\parallel v_\parallel) + \frac{\gamma}{(\omega - k_\parallel v_\parallel)^2 + \gamma^2}\right]k_\parallel\frac{\partial}{\partial v_\parallel}F_e^0 \qquad (4.22)$$

d) RELATIONSHIP WITH EXPERIMENTS

As we shall indicate in Section 7, the non-collisional heating of the ions that occurs in the slide-away regime is well correlated with the onset of the modes treated in this section. In addition, as indicated earlier, we consider the momentum transfer to the ions represented by Eqs (4.18) and (4.19) as preventing the circulating electron distribution from running away as a whole. Finally, we quote Ref.[18] where it has been argued that the process by which this mode saturates involves wave-particle resonances with the ion distribution transverse to the magnetic field. Specifically, as the instability develops and transfers energy to the ions, the width of their distribution increases, and so does the ion Landau damping of the mode until it compensates the rate of energy and momentum absorbed from the current carrying electron distribution. Then, the transverse ion energy can be expected to be proportional to the electron streaming energy and in particular $T_i \propto m_e u_1^2$, which implies $T_i/T_{el} \propto \hat{u}_1^2 \propto \xi^2$, as shown in Fig. 9, where $\hat{u}_1$ is the ratio of the stream velocity of circulating electrons to the thermal velocity v_{the1}, ξ being the average over the plasma cross-section of $J_\parallel/(n e v_{the_1})$ and $J_\parallel$ the measured longitudinal current density.

e) MODES AT THE REDUCED ELECTRON PLASMA FREQUENCY

Experimental observations on Alcator in the slideaway regime (see Section 7) show that modes at frequencies corresponding to $\omega \simeq (k_\parallel/k)\omega_{pe}$(S band) are also excited before, and apparently for values of ξ smaller than those required for the onset of

the fluctuations at ω_{pi}. The higher branch of the dispersion relation (4.9) would give the right frequency range but not the proper value of $\hat{u}_e$, so that a different process should be considered. As a hint, we may use the experimental fact that the reduced electron plasma waves accompany a peak of hard X-ray emission [6], which indicates the presence of runaway electrons. We may thus assume that the most energetic part of the electron distribution tends to develop a tail before the onset of the slide-away regime, as is indicated in Fig.10. The temperature anisotropy of the tail can drive the reduced electron plasma waves unstable through a cyclotron resonance, which would convert longitudinal energy into perpendicular energy [19]. However, as we shall see, the constraints that are imposed on the profile of the electron distribution for the excitation of this mode can be rather severe [20]. Another possibility (Fig.13) which we may consider is that a bump develops in the distribution above the thermal velocity, as most of the circulating electron distribution remains tied to the trapped-electron distribution by the effects of collisions and, possibly, of low-frequency modes [21].

In the limits $k_{\|} v_{the} \ll \omega \simeq \omega_{pe}(k_{\|}/k) \ll |\Omega_e|$ and $b_e < 1$, the relevant dispersion relation, for an electron distribution with a runaway tail, is

$$k^2\lambda_{De}^2 = \tfrac{1}{2} k_{\|}^2 v_{the}^2/\omega^2 + i\mathcal{I} \tag{4.23}$$

where the ion contribution has been neglected and

$$\mathcal{I} = \frac{\pi}{n_e}^2 v_{the}^2 \int d^3v \sum_{n=-\infty}^{\infty} J_n^2(k_\perp v_\perp/\Omega_e)\,\delta(\omega - k_{\|} v_{\|} - n\Omega_e)$$

$$\times \left[k_{\|} v_{\|} \frac{\partial f_e^0}{\partial v_{\|}^2} + n\Omega_e \frac{\partial f_e^0}{\partial v_\perp^2} \right] \tag{4.24}$$

From Eq.(4.23), we have for the real and the imaginary parts of the frequency

$$\omega_0^2 = \left(\frac{k_{\|}}{k}\right)^2 \omega_{pe}^2 \tag{4.25}$$

and

$$\gamma/\omega_0 = \mathcal{I} \frac{\omega_0^2}{k_{\|}^2 v_{the}^2} \tag{4.26}$$

If we choose the solution with $\omega_0 > 0$, the instability condition is

$$\int d^3v\,\delta(\omega - k_{\|} v_{\|}) k_{\|} v_{\|} \frac{\partial f_e^0}{\partial v_{\|}^2} + \sum_{n=\pm 1} \int d^3v\, \tfrac{1}{2} b_e \hat{v}_\perp^2$$

$$\times \delta(\omega - k_{\|} v_{\|} - n\Omega_e) \left[k_{\|} v_{\|} \frac{\partial f_e^0}{\partial v_{\|}^2} + n\Omega_e \frac{\partial f_e^0}{\partial v_\perp^2} \right] > 0 \tag{4.27}$$

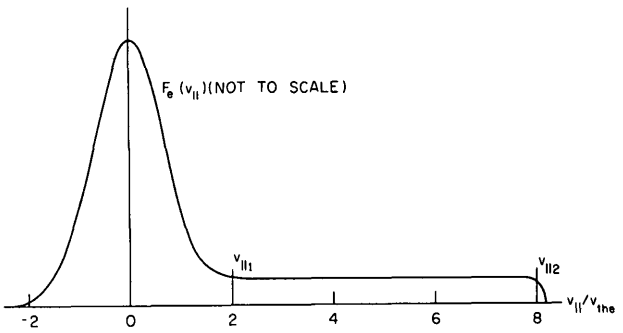

FIG. 10. Model electron distribution function $F_e(v_{\|}) = \int dv_\perp^2 f_e(v_{\|}, v_\perp)$ when the most energetic part of the electron distribution tends to develop a tail, while the remaining electrons are tied together.

where the expansions $J_0^2(k_\perp \rho_e \hat{v}_\perp) \simeq 1$ and $J_1^2(k_\perp \rho_e \hat{v}_\perp) \simeq (b_e/2)\hat{v}_\perp^2$ have been used, and the higher harmonics have been neglected since they are of higher order in b_e. Notice that, in the definition of b_e, $v_{the_\perp} \simeq v_{the}$ (for the body of the distribution) has been assumed. The effective transverse temperature in the tail will, instead, be assumed to be smaller than that of the main body.

For a Maxwellian distribution function with a tail as the distribution function under consideration, the first integral in Eq.(4.27) is always negative.

Since Ω_e is negative we must choose $k_{\|}$ positive so that the resonance condition $k_{\|} v_{\|} = -n\Omega_e + \omega_0 \simeq -n\Omega_e$ can be satisfied in the tail (which is assumed to develop in the positive parallel velocity region) with $n = 1$. Then the $n = 1$ harmonic gives a positive contribution and the $n = -1$ harmonic can be neglected. After integration over $v_{\|}$, neglecting $\partial f_e^0/\partial v_{\|}^2\big|_{v_{\|} = -\Omega_e/k_{\|}}$ compared to $\partial f_e^0/\partial v_\perp^2\big|_{v_{\|} = -\Omega_e/k_{\|}}$, the instability condition becomes

$$\frac{\omega_0}{k_{\|} v_{the}} \int d^2\hat{v}_\perp \left.\frac{\partial f_e^0}{\partial \hat{v}_{\|}^2}\right|_{v_{\|} = \omega_{pe}/k} + \frac{\Omega_e}{k_{\|} v_{the}} \frac{1}{2} b_e$$

$$\times \int d^2\hat{v}_\perp \hat{v}_\perp^2 \left.\frac{\partial f_e^0}{\partial \hat{v}_\perp^2}\right|_{v_{\|} = -\Omega_e/k_{\|}} > 0 \tag{4.28}$$

The first term is equal to $n_e[\omega_{pe}/(k v_{the}\sqrt{\pi})] \times \exp\{-[\omega_{pe}/(k v_{the})]^2\}$, if we assume that the relevant resonance velocity ω_{pe}/k sees the Maxwellian body of the distribution, while the second term is equal to

$$[n_1/(2\sqrt{\pi})][\Omega_e/(k_{\|} v_{the})]$$

where

$$n_1 \equiv v_{the} \sqrt{\pi} \int dv_\perp^2 v_\perp^2 \left.\partial f_e^0/\partial v_\perp^2\right|_{v_{\|} = -\Omega_e/k_{\|}}.$$

Notice that the number density of electrons in the tail of the distribution extending over the interval $\Delta v_{\|} = v_{\|2} - v_{\|1}$, if it is flat in $v_{\|}$, is $n_t \approx n_1(\Delta v_{\|})/v_{the}$, and that the perpendicular temperature of the tail

does not appear in the expression for n_1 we are considering. The instability condition can thus be rewritten as

$$n_1/n_e > 4\left|\Omega_e/\omega_{pe}\right|(k\,k_\parallel/k_\perp^2)\alpha^2\exp\{-\alpha^2\} \qquad (4.29)$$

where $\alpha \equiv \omega_{pe}/(k\,v_{the})$. We also notice that $\Omega_e/k_\parallel < v_{\parallel 2}$, while $\omega_{pe}/k \leq v_{\parallel 1}$. Then $4\left|\Omega_e/\omega_{pe}\right|(k\,k_\parallel/k_\perp^2) > 4\left|\Omega_e^2/\omega_{pe}^2\right|(k/k_\perp)^2 v_{\parallel 1}/v_{\parallel 2}$ and Eq.(4.29) becomes

$$n_1/n_e > 4\left|\Omega_e^2/\omega_{pe}^2\right|(k/k_\perp)^2(v_{\parallel 1}/v_{\parallel 2})\alpha^2\, e^{-\alpha^2}$$
$$> 100(v_{\parallel 1}/v_{\parallel 2})\alpha^2\, e^{-\alpha^2} \qquad (4.30)$$

for $\left|\Omega_e/\omega_{pe}\right| \geq 5$. If we assume for instance $v_{\parallel 1} \simeq 2v_{the}$, and consequently $\alpha \leq 2$, we have $n_1/n_e > 30\,(v_{the}/v_{\parallel 2})$, requiring $v_{\parallel 2} \gg v_{the}$ and giving $n_t/n_e > 30(1 - v_{\parallel 1}/v_{\parallel 2}) \simeq 30$, which is clearly absurd. For larger values of α, we may neglect Landau damping since the n = 0 resonance occurs within the flat tail. Since also the n = 1 resonance has to occur within the tail, we must have $v_{\parallel 2} > \left|\Omega_e\right|/k_\parallel = \left|\Omega_e/\omega_{pe}\right|(k/k_\parallel)\,\alpha > 10\,v_{the}\,(k/k_\parallel)$, for $(\Omega_e/\omega_{pe}) = 5$ and $\alpha > 2$. However, in considering these inequalities, we should take into account the relativistic corrections to the resonant condition (4.24) that are derived in the Appendix. In this case, if we assume $T_e \approx 1$ keV, we would find $v_{\parallel 2}/v_{the} > 10\,k/k_\parallel(1 + 0.41\,k^2/k_\parallel^2)^{-1/2} > 8.4\,v_{the}$, (larger than $14.8\,v_{the}$ for $k = \sqrt{2}\,k_\parallel$). This would require having a significant number of electrons with total energy $m_e c^2\gamma = m_e c^2\,[1 - (v/c)^2]^{-1/2}$ larger than 607 keV, (larger than 1655 keV for $k_\parallel = k/\sqrt{2}$), where $m_e c^2 \simeq 511$ keV.

Less extreme conditions are required, however, if we assume that the region of the electron distribution corresponding to the n = 0 resonance has a less steep slope than the one of the Maxwellian considered above or even a positive slope. Then, for values of $\hat{u}_e$ approaching the threshold value for the $\omega = \omega_{pi}$ instability, a relatively short tail is sufficient to have the reduced electron plasma frequency modes driven by the n = 1 (cyclotron) resonance.

5. ELECTRON LOSS-CONE MODES

a) SIMPLIFIED STABILITY ANALYSIS IN LINEAR GEOMETRY

The following frequency ordering is relevant to a number of magnetic confinement experiments:

$$\langle\omega_t\rangle_i < \langle\omega_t\rangle_e < \Omega_i < \omega_{pi} < \omega_{pe} < \left|\Omega_e\right| \qquad (5.1)$$

where $\langle\omega_t\rangle_j$ is the average transit frequency, ω_{pj} the plasma frequency, and Ω_j the cyclotron frequency for the species j. The electron cyclotron modes, the highest frequency electrostatic modes that can be excited in this case, are expected to become unstable as a result of the depletion of electrons in the left portion of the "loss-cone" in velocity space which has been discussed in Section 2. Since $\omega \gtrsim \left|\Omega_e\right|$, the magnetic moment μ_e is not conserved for these modes and the electrons interacting with them can be scattered into the "loss-cone" of the distribution indicated in Figs 3 and 4.

Since the wavelengths of these modes, both parallel and perpendicular to the magnetic field, are much shorter than the dimensions of the torus, we shall first approximate the dispersion relation as if in a linear geometry and use the electron distribution function derived in Section 2 that is relevant to a spatial region around $\theta = 0$. The θ-dependent corrections to the dispersion relation will be considered later, and will lead us to employ wave packets propagating from the outside of the torus (unstable region) to the inside (stable region), instead of normal modes.

We have simulated the equilibrium electron distribution, of the type described in Section 2, by the following analytical form:

$$f_e^0(v_\parallel, v_\perp) \simeq \frac{n}{\pi^{3/2} v_{the}^3}\left\{H(\hat{v}_\perp^2 - \hat{w}^2)\left[H(2\epsilon_0\,\hat{v}_\perp^2 - \hat{v}_\parallel^2)\right.\right.$$
$$\times e^{-\hat{v}_\parallel^2 - \hat{v}_\perp^2} + H(\hat{v}_\parallel^2 - 2\epsilon_0\,\hat{v}_\perp^2)\,\mathcal{A}\, e^{-a^2\hat{v}_\perp^2 - (\hat{v}_\parallel - \hat{u}_c)^2 + b\hat{v}_\perp^2(\hat{v}_\parallel - \hat{u}_c)/\hat{v}}\Big]$$
$$\left. + H(\hat{w}^2 - \hat{v}_\perp^2)\,\mathcal{A}\, e^{-a^2\hat{v}_\perp^2 - (\hat{v}_\parallel - \hat{u}_c)^2 + b\hat{v}_\perp^2(\hat{v}_\parallel - \hat{u}_c)/\hat{v}}\right\} \qquad (5.2)$$

where u_c is the separation in velocity space between the two electron populations, and is related to the drift velocity u_1 of the circulating electrons; $\hat{u}_c$, $\hat{v}_\perp$, and $\hat{v}_\parallel$ indicate $u_c/v_{the_\parallel}$, $v_\perp/v_{the_\parallel}$, and $v_\parallel/v_{the_\parallel}$ respectively, $v_{the_\parallel}$ the longitudinal electron thermal velocity, $\hat{v} = \{(\hat{v}_\parallel - \hat{u}_c)^2 + \hat{v}_\perp^2\}^{1/2}$, H is the Heaviside function, $\mathcal{A}$ is an ad hoc normalization factor, a^2 and b give respectively $T_{e\parallel}/T_{e\perp}$ and the magnitude of the triangular deformation of the circulating electron distribution, and $\hat{w}$ is the lower cut-off on $\hat{v}_\perp$ for the trapped electrons. For numerical computations at $\hat{u}_c = 1$, $a^2 = 1.34$, b = 0.88, $\hat{w} = 0.01$ and $\mathcal{A} = 0.78$ have been used.

To illustrate the instability mechanism, the limit $u_c \gg v_{the}$, that corresponds to a pie-slice-shaped distribution in velocity space $(v_\parallel, v_\perp)$, will be studied analytically, while the distribution (5.2) will be adopted in deriving the numerical results presented in this section. The relevant dispersion relation, neglecting the ion contribution, can be written as [22]:

$$k^2 = -8\pi^2\,\frac{e^2}{m_e}\sum_m \int_0^\infty dv_\perp^2 \int_{-\infty}^{+\infty} dv_\parallel$$
$$\times \frac{J_m^2(k_\perp v_\perp/\Omega_e)}{\omega - k_\parallel v_\parallel - m\Omega_e}\left[\frac{k_\parallel}{2}\,\frac{\partial f_e^0}{\partial v_\parallel} + m\Omega_e\,\frac{\partial f_e^0}{\partial v_\perp^2}\right] \qquad (5.3)$$

where $\Omega_e = -eB/(m_e c) < 0$. We consider $k \sim k_\perp$ and $b_e = (1/2)\,k_\perp^2\rho_e^2 \sim 1$, where ρ_e is the average

electron gyroradius. Then $k^2\lambda_{De}^2 > 1$ and, considering explicitly the m = 1 harmonic, we have $\omega = \Omega_e + \delta\omega$, where $\delta\omega/|\Omega_e| \sim \omega_{pe}^2/\Omega_e^2$. If we consider $k_\parallel v_\parallel \sim \delta\omega$, we may argue that the first term in square brackets is smaller than the second one by the order of $\delta\omega/|\Omega_e|$.

In the case of a pie-slice-shaped electron distribution, the existence of a marginal stability condition can be shown easily: we only need to prove that a real $\delta\omega$ exists such that $\mathrm{Im}\,\epsilon = 0$, where ϵ is the dielectric constant,

$$\mathrm{Im}\,\epsilon\Big|_{\omega_{real}} \propto \int_0^\infty J_1^2\, dv_\perp^2 \left.\frac{\partial f_e^0}{\partial v_\perp^2}\right|_{v_\parallel = v_{res}} \tag{5.4}$$

where $v_{res} = \delta\omega/k_\parallel$,

$$\left.\frac{\partial f_e^0}{\partial v_\perp^2}\right|_{v = v_{res}} \propto e^{-\hat{v}_\perp^2}\left[\delta(\hat{V}^2 - \hat{v}_\perp^2) - H(\hat{V}^2 - \hat{v}_\perp^2)\right] \tag{5.5}$$

and $\hat{V}^2 = (\delta\omega/k_\parallel v_{the})^2/(2\epsilon_0)$, so that

$$\mathrm{Im}\,\epsilon\Big|_{\omega_{real}} \propto J_1^2(b_e\hat{V}^2)\, e^{-\hat{V}^2} - \int_{\hat{V}^2}^\infty J_1^2\, e^{-\hat{v}_\perp^2}\, d\hat{v}_\perp^2 \tag{5.6}$$

where $b_e = (1/2)\,k_\perp^2\rho_e^2$ and ρ_e is the electron gyroradius. When $b_e\hat{V}^2$ coincides with a zero of the Bessel function, then $\mathrm{Im}\,\epsilon < 0$; when instead $b_e\hat{V}^2$ coincides with a maximum, then $\mathrm{Im}\,\epsilon > 0$, since J^2 has monotonically decreasing maxima. By continuity, a b_e exists such that $\mathrm{Im}\,\epsilon = 0$. In the limits $|\gamma| = |\mathrm{Im}\,\delta\omega| < |\delta\omega|$ and $|k_\parallel v_{the}| < |\delta\omega| < |\Omega_e|$, an approximate solution of the dispersion relation (5.3) is, writing $\delta\omega_0 = \mathrm{Re}\,\delta\omega$,

$$\frac{\delta\omega_0}{\Omega_e} = \frac{-2\pi\omega_{pe}^2}{nk^2}\int_0^\infty dv_\perp^2 J_1^2 \int_{-\infty}^{+\infty} \frac{\partial f_e^0}{\partial v_\perp^2}\, dv_\parallel \tag{5.7}$$

and

$$\gamma = -\pi\,\frac{\delta\omega^2}{|k_\parallel|}\,\frac{\int_0^\infty dv_\perp^2 J_1^2 \left.\frac{\partial f_e^0}{\partial v_\perp^2}\right|_{v_\parallel = v_{res}}}{\int_0^\infty dv_\perp^2 J_1^2 \int_{-\infty}^{+\infty} \frac{\partial f_e^0}{\partial v_\perp^2}\, dv_\parallel} \tag{5.8}$$

where γ is given by the wave-particle resonance. The function $\int_{-\infty}^{+\infty} (\partial f_e^0/\partial v_\perp^2)\, dv_\parallel$ is sketched in Fig.11 with $\epsilon_0 = 0.25$ and the choice of characteristic parameters indicated below Eq.(5.2).

In Fig.12, the numerical results for $\hat{v}_{res} = -1.5$ are shown in the interval of values of b_e which are compatible with the assumption $|\delta\omega/k_\parallel| > v_{the}$, and taking $k_\parallel \simeq k_\perp\epsilon_0/q$ that is consistent with

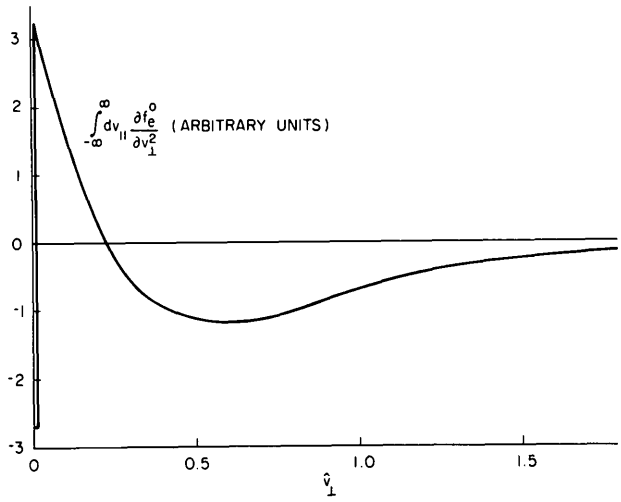

FIG. 11. The quantity $\int_{-\infty}^{\infty} dv_\parallel (\partial f_e^0/\partial v_\perp^2)$ as a function of $\hat{v}_\perp = v_\perp/v_{the}$ which occurs in connection with the electron cyclotron modes, Eqs (5.7, 8).

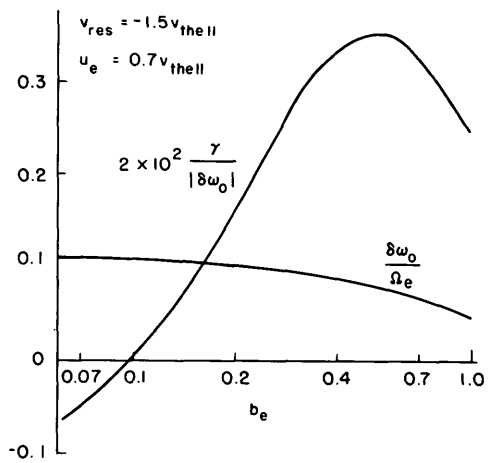

FIG. 12. Real frequency and growth rate for electron cyclotron modes as functions of $b_e = (1/2)\,k_\perp^2\rho_e^2$, where ρ_e is the electron gyroradius, in the limit $(\omega - \Omega_e)/k_\parallel \equiv v_{res} < -v_{the\parallel}$ where the expressions (5.7) and (5.8) are valid.

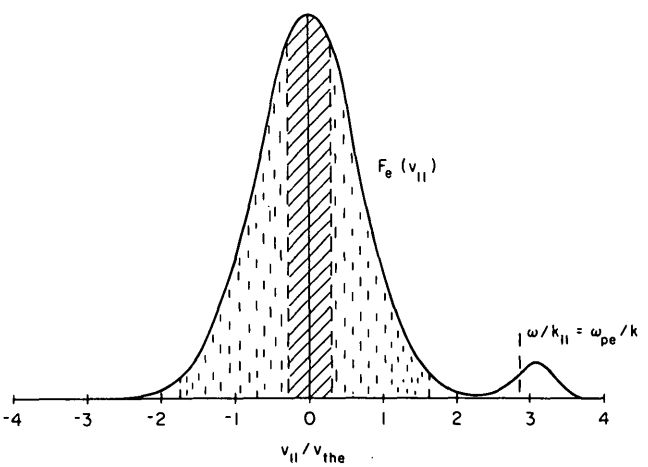

FIG. 13. Model electron distribution function $F_e(v_\parallel) \equiv \int d^2 v_\perp f_e(v_\parallel, v_\perp)$ under the assumption that, as a result of collisions and of collective modes, a considerable part of the electron distribution remains tied to the trapped portion of it, so that only a small fraction, in the distribution tail, is allowed to run away as a whole.

the toroidal geometry described in Section 3. The mode is unstable when the integral in the numerator of Eq.(5.8) becomes positive as a result of the coincidence between a maximum of the Bessel function and the discontinuity in the resonant contribution. In the considered interval of b_e, the integral in the denominator of Eq.(5.8) is negative and thus $\delta\omega/\Omega_e$ is positive and $k_\parallel$ negative. Moreover, the energy of the unstable waves is positive [13]:

$$\mathcal{E} = \sum_{\vec{k}} |E_{\vec{k}}|^2 \frac{\omega}{8\pi} \frac{\partial \epsilon}{\partial \omega} \simeq \sum_{\vec{k}} |E_{\vec{k}}|^2 \frac{\Omega_e}{8\pi} \frac{\partial \epsilon}{\partial \delta\omega}$$

$$= \sum_{\vec{k}} |E_{\vec{k}}|^2 \frac{\Omega_e}{\delta\omega 8\pi} = - \sum_{\vec{k}} |E_{\vec{k}}|^2 \frac{k^2 n}{16\pi^2 \omega_{pe}^2}$$

$$\times \left[\int_0^\infty dv_\perp^2 J_1^2 \int_{-\infty}^{+\infty} \frac{\partial f_e^0}{\partial v_\perp^2} \, dv_\parallel \right]^{-1} \qquad (5.9)$$

This result is still valid for considerably smaller values of $k_\parallel/k$ than 1/10 that correspond to $\epsilon_0 < 1/4$ and $q > 2.5$. A more complete analysis of the instability condition can be carried out numerically substituting Eq.(5.2) into Eq.(5.3) and looking for the condition of marginal stability for different values of v_{res}, b_e, and $\hat{u}_c$. The characteristic result is a threshold value for $\hat{u}_c$ ranging between 1.0 and 1.2, which implies $u_e \equiv -(J/ne) \simeq 0.4\, v_{the}$ for $R_0/r \sim 4$ and $u_e \simeq 0.8\, v_{the}$ for $R_0/r \sim 16$. Note that these values are larger than those quoted for the experiments discussed in Section 7. In addition, we notice that a more realistic model of the equilibrium distribution, including the effects of collisions, would link the formation of a loss-cone feature in the distribution to the average drift velocity of the circulating particles in a different way from the one we have chosen to consider. In this collisional case, the role of more energetic electrons is enhanced and the values of u_e, for which the excitation of the considered loss-cone modes can be predicted, should be smaller than those indicated earlier.

As a consequence of the excitation of the electron loss-cone modes, we expect that, in the negative parallel velocity region of the electron distribution function, a new equilibrium is set up. In this situation, the pitch angle scattering produced by these modes is compensated by the decrease of $|v_\parallel|/v_\perp$ produced by the external electric field E_0. These two processes appear in the quasi-linear equation for the evolution of the average electron distribution function:

$$\frac{\partial f_e^0}{\partial t} - \frac{e}{m_e} E_0 \frac{\partial f_e^0}{\partial v_\parallel}$$

$$= i \sum_{\vec{k}} \frac{e^2}{m_e^2} \frac{|E_{\vec{k}}|^2}{k^2} \left[\frac{\Omega_e}{v_\perp} \frac{\partial}{\partial v_\perp} + k_\parallel \frac{\partial}{\partial v_\parallel} \right]$$

$$\times \frac{J_1^2(k_\perp v_\perp/\Omega_e)}{\omega_k - k_\parallel v_\parallel - \Omega_e} \left[\frac{\Omega_e}{v_\perp} \frac{\partial}{\partial v_\perp} + k_\parallel \frac{\partial}{\partial v_\parallel} \right] f_e^0(v_\perp, v_\parallel) \qquad (5.10)$$

On the right-hand side, the prevailing term, $(\Omega_e/v_\perp)(\partial/\partial v_\perp)$, describes the perpendicular diffusion in velocity space that tends to fill the "loss cone" while the term $k_\parallel(\partial/\partial v_\parallel)$ corresponds to a transfer of parallel momentum within the electron distribution. On the left-hand side, the term $E_0(\partial f_e^0/\partial v_\parallel)$ describes the change in $v_\parallel$ due to the electric field. We could then use Eq.(5.10) to evaluate an effective collision frequency that is relevant to the present problem. For this, we may simplify Eq.(5.10) to the form

$$\frac{\partial f_e^0}{\partial t} - \frac{e}{m_e} E_0 \frac{\partial f_e^0}{\partial v_\parallel} = \sum_{\vec{k}} \left| \frac{e\phi_{\vec{k}}}{T_e} \right|^2 \Omega_e^2 v_{the}^4$$

$$\times \frac{\partial}{\partial \hat{v}_\perp^2} J_1^2 \left(\frac{\gamma}{\delta\omega_0^2} + \pi\delta(\delta\omega_0 - k_\parallel v_\parallel) \right) \frac{\partial}{\partial \hat{v}_\perp^2} f_e^0$$

where the relevant diffusion coefficient $\mathcal{D}_{v_\perp v_\perp}$ can be rewritten as

$$\frac{\mathcal{D}_{v_\perp v_\perp}}{v_{the}^4} \approx \sum_{\vec{k}} \left| \frac{e\phi_{\vec{k}}}{T_e} \right|^2 J_1^2 \Omega_e^2$$

$$\times \left(\frac{\gamma}{\delta\omega_0^2} + \pi\delta(\delta\omega_0 - k_\parallel v_\parallel) \right)$$

which is of order

$$\sum_{\vec{k}} \left| \frac{e\phi_{\vec{k}}}{T_e} \right|^2 \frac{\Omega_e^2}{\delta\omega_0^2} \gamma$$

b) CONVECTIVE MODES

Toroidal geometry introduces θ-dependent corrections to the solution of the dispersion relation given by Eq.(5.3). To compute these corrections we make use of the results in Section 3. We factorize the θ-dependence of the potential of the mode into a fast-varying complex exponential multiplied by a slow function $\tilde{\phi}_{m_0, n_0}$ which describes the envelope of the mode. The wave numbers $k_\perp$ and $k_\parallel$ are replaced by the operators $k_r \to -(i/r)\partial/\partial\theta$ and $n^0/R_0 \to -(i/qR_0)\partial/\partial\theta$, respectively, and $\delta\omega$ is the sum of two terms $\delta\omega = \delta\omega_1 + \delta\omega_2$, where $\delta\omega_1$ is given by Eq.(5.7) and $\delta\omega_2$ is the correction due to the θ-dependence. If we expand the dispersion relation up to second-order derivatives in θ and second-order terms in θ around $\theta = 0$, and if we subtract the θ-independent contribution, we obtain the equation

$$-\left(\frac{1}{q^2R_0^2}+\frac{1}{r^2}\right)\frac{\partial^2}{\partial\theta^2}\,\tilde{\phi}_{m^0,n^0}+k^2\,\frac{\delta\omega_2}{\delta\omega_0}\,\tilde{\phi}_{m^0,n^0}$$

$$=-\frac{2\pi\omega_{pe}^2}{n}\int_0^{\infty}dv_\perp^2\int_{-\infty}^{+\infty}dv_\parallel$$

$$\times\left\{\left[-(J_1^2)'\,\frac{k_\perp v_\perp}{\Omega_e}\,\frac{\epsilon_0}{2}\,\theta^2\right.\right.$$

$$-(J_1^2)''\,\frac{v_\perp^2}{\Omega_e^2}\,\frac{1}{r^2}\,\frac{\partial^2}{\partial\theta^2}+J_1^2\,\frac{\Omega_e}{\delta\omega}\,\frac{\epsilon_0}{2}\,\theta^2\Big]/\delta\omega$$

$$\times\left[\frac{k_\parallel}{2}\,\frac{\partial f_e^0}{\partial v_\parallel}+\Omega_e\,\frac{\partial f_e^0}{\partial v_\perp^2}\right]$$

$$+\frac{J_1^2}{\delta\omega}\left[\frac{v_\parallel}{2\delta\omega}\,\frac{\partial f_e^0}{\partial v_\parallel}+\frac{\Omega_e v_\parallel^2}{\delta\omega^2}\,\frac{\partial f_e^0}{\partial v_\perp^2}\right]$$

$$\left.\times\,\frac{1}{q^2R_0^2}\,\frac{\partial^2}{\partial\theta^2}+\frac{J_1^2}{\delta\omega}\,A\Delta f\right\}\tilde{\phi}_{m^0,n^0}\qquad(5.11)$$

where a prime on J_1^2 indicates a derivative with respect to the argument, first derivatives with respect to θ have been neglected since, as can be shown, they do not change the nature of the solution, $A\Delta f$ is the term produced by the θ-dependence of the equilibrium distribution function which is of order $\epsilon_0^{1/2}$ (since the number of trapped particles scales like $\epsilon_0^{1/2}$); all quantities are computed at $\theta = 0$ and $k_\perp$ and $k_\parallel$ are defined by Eq.(3.12). Since $r \ll qR_0$, the θ-derivatives coming from $k_\perp$ are more important than those coming from $k_\parallel$. Of the two remaining θ-derivatives, it turns out numerically that the leading one is that derived from the Laplacian (left-hand side of Eq.(5.11)). The leading θ^2-term is the one coming from the expansion of the resonant denominator which is proportional to $\epsilon_0\,\Omega_e/\delta\omega > \epsilon_0^{1/2}$. Thus we obtain the following differential equation:

$$\frac{1}{r^2}\,\frac{\partial^2\tilde{\phi}_{m^0,n^0}}{\partial\theta^2}-k^2\,\frac{\delta\omega_2}{\delta\omega_0}\,\tilde{\phi}_{m^0,n^0}$$

$$\simeq 2\pi\,\frac{\theta^2}{n\lambda_{De}^2}\,\epsilon_0\left(\frac{\Omega_e}{\delta\omega}\right)^2\tilde{\phi}_{m^0,n^0}\int d^3\hat{v}\,J_1^2\,\frac{\partial f_e^0}{\partial\hat{v}_\perp^2}$$

$$=-\epsilon_0 k^2\left(\frac{\Omega_e}{\delta\omega}\right)\theta^2\tilde{\phi}_{m^0,n^0}\qquad(5.12)$$

Owing to the relative signs of the θ^2 and $\partial^2/\partial\theta^2$ terms, Eq.(5.12) has no localized solutions around $\theta = 0$. Thus, instead of considering normal modes, we are led to consider wave packets which originate in the instability region ($\theta \simeq 0$) and migrate towards the inside of the torus ($\theta \simeq \pi$) where the mode is damped as there is no loss cone in the electron distribution. Evaluating the perpendicular group velocity from the numerical solutions of Eq.(5.7), we find, from the results shown in Fig.14, $v_{\perp gr} \simeq 3\times10^{-2}\,v_{the} \simeq 6\times10^7\,\mathrm{cm\cdot s^{-1}}$ for $T_e \simeq 1$ keV. Assuming that the wave packet travels 10 ÷ 20 cm before leaving the unstable region and deriving γ from the numerical results ($\gamma \simeq 10^8\,\mathrm{s^{-1}}$), we find roughly that $\gamma\tau_0 \simeq 16 - 32$, where τ_0 is the time required for the wave packet to escape from the unstable region, which allows the mode to grow significantly.

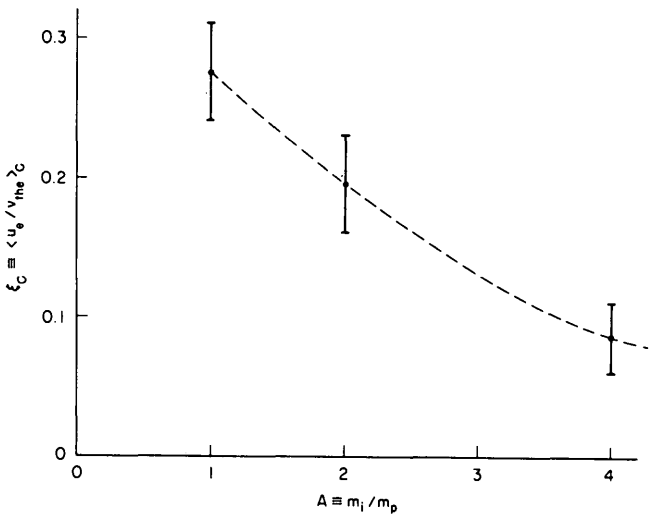

FIG. 14. Dependence on the mass ratio $A \equiv m_i/m_p$, where m_p is the proton mass, of the threshold value ξ_C of $\xi = \langle u_e/v_{the}\rangle$, defined by Eq.(7.1), below which the electron distribution is a Maxwellian with a unique perpendicular temperature and above which it is characterized by two perpendicular temperatures (deduced from Ref.[6]).

6. ION CYCLOTRON MODES, CIRCULATING AND TRAPPED ELECTRON MODES

Ion cyclotron modes, with frequency $\omega \simeq n\Omega_i$, where n is an integer, can be shown in a linearized theory to be destabilized by the current carried by the electrons if the modes resonate in the region of velocity space where the electron distribution function has a positive slope. The portion of the electron population which does not carry any appreciable fraction of the current, i.e. the trapped and quasi-circulating electrons, will tend instead to damp these modes. Referring to the question of energy and momentum transfer to the ions, it appears difficult to find a range of parameters such that the ion cyclotron mode can have an effective resonant interaction with the ions and at the same time be destabilized by the electrons. This is due to the fact that in a torus the corresponding eigenmodes are peaked at the minimum of the magnetic field ($\theta = 0$), and are easily damped by the trapped electrons. A detailed analysis of these questions is given in Ref.[8].

Then we consider modes with frequency ω such that $\langle\omega_t\rangle_i < \langle\omega_b\rangle_e < \langle\omega_t\rangle_e \lesssim \omega < \Omega_i < |\Omega_e|$, and which are localized along a given magnetic field line around the point of minimum or maximum magnetic field.

Their spectrum in parallel-wave-number space has a width which is inversely proportional to the θ-localization width, and is centered at zero, if

the mode is standing, or at $\bar{k}_{\parallel}$ if the mode is localized but travelling, where $\bar{k}_{\parallel}$ gives the central parallel wave number of the oscillations inside the localized envelope of the mode amplitude. Modes of this type are important in that they can resonate with both the highly circulating (current-carrying) electrons and the trapped electrons. Thus, energy and momentum are transferred from the current-carrying to the trapped electrons, and momentum is eventually transferred to the magnetic field from the trapped electrons and from the mode which is "locked-in" with the magnetic field [23, 24]. In particular, it is possible to reach a condition of marginal stability without forming a plateau in the electron distribution.

With respect to standing modes in the frequency range $\langle \omega_t \rangle_i < \omega < \langle \omega_b \rangle_e < \langle \omega_t \rangle_e$, it is difficult to see how they could contribute significantly to anomalous resistivity, since their dominant resonant interaction is with the trapped and barely circulating electrons, which do not carry any appreciable current.

7. RELATIONSHIP WITH EXPERIMENTAL OBSERVATIONS

i) "NEARLY-CLASSICAL", "INTERMEDIATE", AND "SLIDE-AWAY" REGIMES

We shall refer to experiments carried out on the Alcator device [6], as this is one of the few apparatus realized so far in which it is possible to reproduce, under controllable conditions,

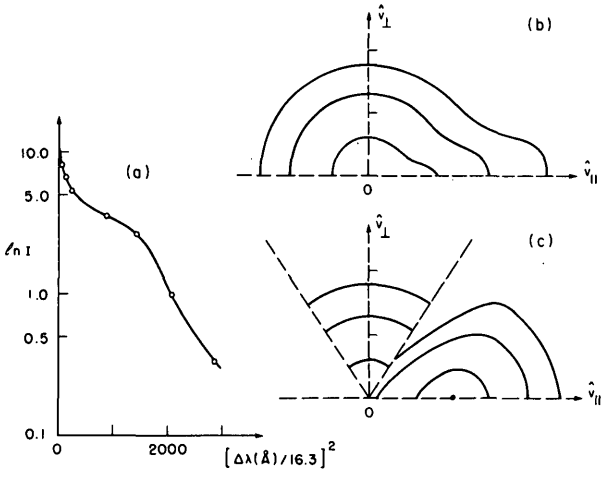

FIG. 15. (a) "Slide-away" electron distributions, integrated over $v_\parallel$, obtained from the spectrum of scattered light intensity versus wave-length shift $\Delta\lambda$ (after Refs [25, 26]).
(b) Inferred electron distribution from the measurements indicated in Fig. 15a), relevant to the "slide-away" regime. Here $\hat{v}_\perp = v_\perp/v_{the}$ and $\hat{v}_\parallel = v_\parallel/v_{the}$.
(c) Theoretical model of a "slide-away" distribution obtained as in Section 2 by assuming that particles with $|v_\parallel/v_\perp| < 0.82$ are magnetically trapped, for $\epsilon_0 \equiv r/R_0 = 0.25$, and neglecting collisions. The initial distribution is a Maxwellian. The transverse temperature of the current-carrying electron distribution is observed to be smaller than that of the original Maxwellian and of the trapped-electron distribution.

electron distributions that are either close to a Maxwellian or distorted from it, while the theoretical conditions for the presence of a considerable fraction of trapped electrons are satisfied. The interval of average electron densities that has been explored is $\bar{n} = 2 \times 10^{12} - 4 \times 10^{14} \cdot \text{cm}^{-3}$, while plasma currents in the range 20 - 200 kA have been realized. The observations to which we refer here are for mean current densities in the range 300 - 500 $\text{A} \cdot \text{cm}^{-2}$. These observations have indicated that we can distinguish three different regimes on the basis of the profile of the transverse electron distribution, as obtained from Thomson scattering experiments, and of the resistivity η referred to the Spitzer-Härm resistivity η_{cl}.

The electron distribution function integrated over $v_\parallel$, that is $\bar{f}_e(v_\perp, \vec{r}) = \int dv_\parallel f_e(v_\perp, v_\parallel, \vec{r})$, has been measured by Thomson scattering mostly at the centre of the plasma toroidal chamber, whose major radius is $R_0 = 54$ cm, and at two points on the equatorial plane with a distance $R = R_0 \pm 3.8$ cm from the symmetry axis. The distribution $\bar{f}_e$ has been observed to be a Maxwellian with a unique temperature $T_{e\perp}$ for $\xi \equiv \langle u_e/v_{the} \rangle \ll \xi_C$, where ξ_C is a reference value of ξ. When $\xi \geq \xi_C$, $\bar{f}_e$ differs from a single Maxwellian and in most cases can be characterized by two temperatures $T_{\perp C} < T_{\perp T}$ [6,25,26] although it is not possible, in general, to reproduce it as a simple superposition of Maxwellians. In particular, the average $\xi \equiv \langle u_e/v_{the} \rangle$ is defined as

$$\left\langle \frac{u_e}{v_{the}} \right\rangle = \frac{2}{a_c^2} \int_0^{a_c} dr\, r \left[\frac{J_\parallel(r)}{en(r)} \right] \left[\frac{2T_e(r)}{m_e} \right]^{-1/2} \tag{7.1}$$

where a_c is the radius of the current channel and T_e is arbitrarily identified with $T_{\perp T}$ when $\xi > \xi_C$. As for the radial profiles appearing in the integral (7.1), it has been assumed that $T_e = T_e(0) \times [1 - (r/a_c)^{3/2}]$, $n = n(0)[1 - (r/a_1)^2]$ and $J_\parallel(r) \propto T_e^{3/2}(r)$, where a_1 is the limiter radius, noticing that the assumed $T_e(r)$ and $n(r)$ appear to be reasonably consistent with the measurements performed at the points specified earlier for densities larger than $3 - 4 \times 10^{13} \cdot \text{cm}^{-3}$. We also notice that, for $\xi > \xi_C$, measurements of soft X-ray spectra indicate the presence of an electron component with energies larger than thermal, so that the average longitudinal electron temperature can be considered to be larger than $T_{\perp T} > T_{\perp C}$. For this reason and since most of the current is expected to be carried by the electron component with the largest average energy, the considered evaluation of ξ, for $\xi > \xi_C$, is not as meaningful as for $\xi < \xi_C$. The threshold ξ_C has been observed to depend on the type of filling gas that has been studied with $\xi_C(H_2) > \xi_C(D_2) > \xi_C(He)$, and has values in the range 0.1 to 0.3, as is shown in Fig.14. The average for the ratio of the longitudinal electrical resistivity $\eta_\parallel$ to the classical resistivity η_{cl},

$$\left\langle \frac{\eta_{\parallel}}{\eta_{cl}} \right\rangle = \frac{2E_{\parallel}}{a_c^2} \int_0^{a_c} dr \, \frac{r}{\eta_{cl}(r) J_{\parallel}(r)} \qquad (7.2)$$

has been evaluated by assuming the same profiles as for (7.1) and $E_{\parallel} \approx$ constant, as a function of r.

The dependences of the transverse electron distribution $\bar{f}_e(v_\perp)$ and the onset of high-frequency fluctuations allow us to distinguish three regimes:

(I) A "nearly-classical" regime for $\xi < \xi_L$ where $\langle \eta_{\parallel}/\eta_{cl} \rangle$ is not a decreasing function of ξ, while the observed $\bar{f}_e(v_\perp)$ is close to a Maxwellian.

(II) An "intermediate" regime [27] for $\xi_L < \xi < \xi_C$ where the observed $\bar{f}_e(v_\perp)$ is Maxwellian but $\langle \eta_{\parallel}/\eta_{cl} \rangle$ decreases as a function of ξ. No high-frequency fluctuations are observed in this regime except for electron cyclotron emission for ξ nearing ξ_C [28]. We envision this regime as being described by a distribution function of the type discussed in Section 2, where the circulating electron distribution is sufficiently stretched that the friction of the current-carrying electrons is considerably decreased with respect to that allowed by the limits of the classical theory, but not sufficiently deformed to develop a region of positive slope. A loss-cone feature in the electron distribution appearing for $\xi \sim \xi_C$ may be responsible for the observed sudden enhancement, as a function of ξ, of the electron cyclotron emission.

(III) A "slide-away" regime characterized by the excitation of high-frequency fluctuations indicated by strong e.m. emission around ω_{pi} as well as at higher frequencies up to the electron cyclotron frequency range [28]. The emission at ω_{pi} is well correlated with the drastic enhancement of ion heating, as a function of ξ, up to temperatures of about 1.2 keV.

In particular, we recall that, in the first two regimes, corresponding to $\xi < \xi_C$, in addition to Thomson scattering observation of a Maxwellian-transverse-distribution, soft-X-ray spectra between 2 and 10 keV show the presence of a nearly thermal tail. Hard X-rays can hardly be detected. The value of ξ_L has not been precisely identified, as yet. However, we notice that a decreasing $\langle \eta_{\parallel}/\eta_{cl} \rangle$, as a function of ξ, has been observed for $\xi > 0.02$, in H_2 plasmas [27].

In the slide-away regime (see Fig.15), the transverse electron distribution indicates that an appreciable fraction of the electron population has a mean transverse energy $T_{\perp C}$ smaller than that ($T_{\perp T}$) of the rest as pointed out earlier, and soft X-ray spectra show an enhanced tail between 2 and 5 keV. Moreover, some hard X-rays have been detected by a scintillator, but the measured dose near the plasma limiter, by employing a commercial dosimeter, is less than 1 mR for a duration of the plasma current pulse of about 100 ms. We notice that in plasma discharges where a considerable number of runaways are present, the corresponding measured dose is about 500 mR. Another important phenomenon observed in the "slide-away" regime is the drastic increase of the ion temperature as ξ reaches a threshold value ξ_C, as we have mentioned earlier. Notice that when maintaining the plasma current constant while varying the density, ξ can be increased by decreasing the density n. In these conditions, while in regimes I and II that are more collision dominated T_i is seen to increase with n, as the rate of electron-ion collisional energy transfer increases, in regime III the contrary occurs. The onset of anomalous ion heating is well correlated with an electromagnetic signal that is sharply peaked at a frequency between 350 and 700 MHz and extends with a continuous spectrum up to 4 GHz [10]. A typical emission spectrum is shown in Fig.16. This signal is collected from a segment of the metallic limiter that is kept floating, or from a metallic probe that is placed in the shadow of the plasma limiter. The frequency at which the spectrum is peaked has been identified (see Fig.17) with $\omega_{pi} = (4\pi ne^2/m_i)^{1/2}$, and we have connected this with a mode driven by the current-carrying electron distribution, as described in Section 4. The dependence of the emitted power at this frequency on ξ is shown in Fig.18. No measurements between 4 GHz and 150 GHz, where the electron cyclotron emission begins for $B \approx 50$ kG, have been carried out. In this connection, we recall that previous experiments carried out on the CLEO device [7] have led to the observation of cyclotron emission well above the thermal level, and this was attributed to the presence of a significant concentration of runaway electrons. This explanation, however, requires also that a process for the pitch angle scattering of electrons with velocity parallel to the

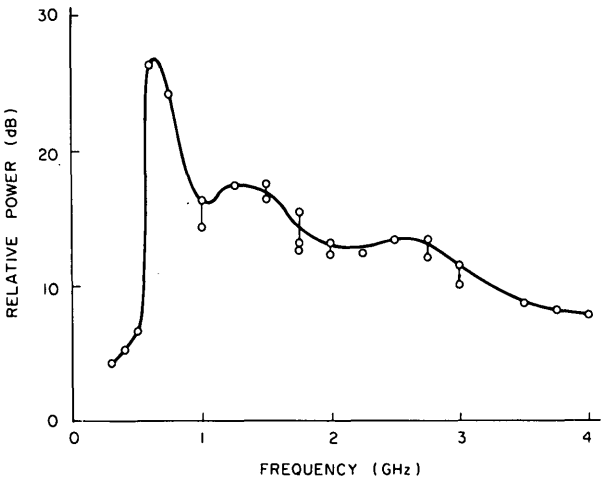

FIG. 16. Spectral emission from a hydrogen plasma at 20 ms, with shot-to-shot measurements taken at various fixed frequencies, and with I = 100 kA, B_0 = 40 kG, $n_e = 9 \times 10^{12}$ cm^{-3} (after Ref. [10]).

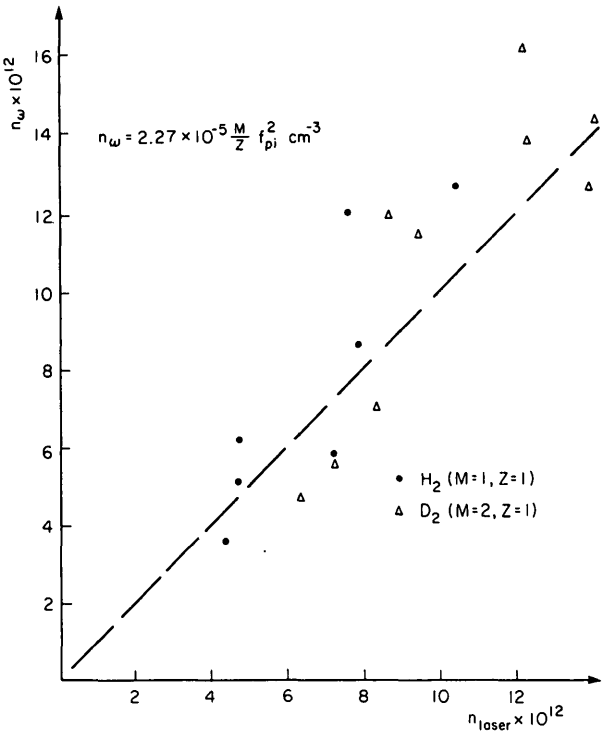

FIG. 17. Comparison of the average plasma density as obtained from Thompson scattering, and from the assumption that the peak emission of electromagnetic noise has a frequency about equal to the ion plasma frequency $\omega_{pi} = (4\pi ne^2/m_i)^{1/2}$, for hydrogen and deuterium (from Ref. [10]).

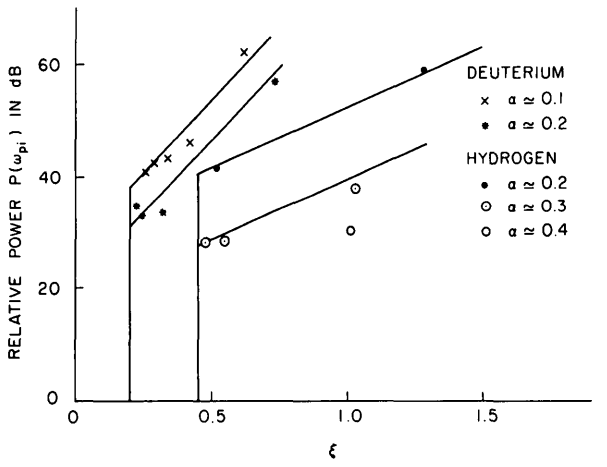

FIG. 18. Relative power level P of the radiation emitted at $\omega_{pi} = (4\pi ne^2/m_i)^{1/2}$ versus $\xi = \langle u_e/v_{the} \rangle$, defined in Eq. (7.1), at various impurity levels characterized by $\alpha \equiv Z^2 n_I/n$, where Z is the impurity charge number and $n_I < n$ is the impurity number density (after Ref. [10]).

magnetic field be indicated. In particular, if the one represented by the dispersion relation (4.23) is considered, there are a number of conditions to satisfy for the relevant instability as indicated at the end of Section 4.

Now, we notice that the excitation of fluctuations with frequencies around 2.4 GHz has been detected to precede the onset of the mode at ω_{pi} and to coincide with the emission of a burst of hard X-rays. In addition, no measurements of fluctuations that may be excited at the electron transit frequency or below it have been made as yet. Finally, we point out that the collisional resistivity would be zero in the slide-away regime, and we consider the modes treated in Section 4 as being responsible for keeping $\eta_\parallel$ finite.

ii) THE ELECTRICAL RESISTIVITY PROBLEM

We notice that the expected values of $\eta_\parallel$ depend, in general, on a number of parameters, besides ξ, such as $E_\parallel/E_R$, the (average) charge and mass numbers of the ion species, and Υ_e that indicates the extent to which a fraction of the electron population can have magnetically trapped orbits. Thus $\Upsilon_e = \langle \omega_b \rangle_e / [(R_0/r)\nu_{ei}]$, where $\langle \omega_b \rangle_e$ is the average bounce frequency of trapped electrons and we have, numerically, $\Upsilon_e \approx (\hat{r}/\hat{R})^{3/2} \times \{\hat{T}_e^2(r)/[\hat{n}(r)(Z\,\hat{q}\,\hat{R}\,\hat{\lambda})]\} \times 10^2$, where $\hat{T}_e$ is the electron temperature in keV, $\hat{n}$ the electron density in $10^{13} \cdot \text{cm}^{-3}$, $\hat{\lambda} = (\ln \Lambda)/(15)$ is a measure of the well known Coulomb logarithm, $\hat{R} = R_0/(50\text{cm})$, $\hat{r} \equiv r/(10\text{cm})$, $\hat{q} = q/(2.5)$, and Z is the ionic charge number.

We recall that the collisional theory of resistivity, applied for $\Upsilon_e \gg 1$ and assuming $E_\parallel/E_R$ sufficiently low that the Spitzer-Härm approximation [1] can be made, would predict $\langle \eta_\parallel/\eta_{cl} \rangle$ to be larger than unity [11]. However, we may not consider this prediction as valid for regimes II and III where we can argue that the current is mostly carried by sufficiently fast electrons whose decreased friction more than compensates the decrease in the number of carriers.

We point out that while in a strongly collisional regime, for a given electron temperature, $\eta_\parallel$ is determined only by the longitudinal electron momentum balance equation, in regimes II and III, where $\eta_\parallel < \eta_{cl}$, the electron thermal energy balance equation has a direct influence on the expression for $\eta_\parallel$ [29]. In particular, the condition for the onset of regime II is met when the applied electric field $E_\parallel$ reaches a critical value, that is a fraction of E_R, at which the collisional friction of a significant part of the electron population with the ions and with the remaining electron population is no longer sufficient to prevent it from being continuously accelerated [29-31]. As a result, the electron distribution will be increasingly "stretched" in the direction of acceleration, and the average kinetic energy content of the total electron distribution will also increase. The maximum "stretching" is therefore limited by the electron "thermal" energy balance equation and the value of u_e that is reached in the stationary state is determined by this equation as well as by that for longitudinal momentum balance. If we write the expression for resistivity in terms of the dimensionless parameters, $E_\parallel/E_R$ and u_e/v_{the} as indicated earlier, we have $\eta_\parallel = E_\parallel/J_\parallel = (E_\parallel/E_R)(v_{the}/u_e) A_T \eta_{cl} (2/\Phi(Z))$, where $\Phi(Z)$ is a function which is tabulated in Ref. [32], and A_T indicates the increase of resistivity due to the magnetic

trapping of a fraction of the electron population. If we assume that the intermediate regime corresponds to $E_{\parallel}/E_R$ reaching a value α_E for which a considerable fraction of the electron population tends to runaway as a whole, we have

$$\frac{\eta_{\parallel}}{\eta_{cl}} = \frac{2\alpha_E}{\Phi(Z)} \left(\frac{v_{the}}{u_e}\right) A_T \qquad (7.3)$$

and this grossly represents the trend of $\eta_{\parallel}/\eta_{cl}$ indicated by the experimental observations. To evaluate ξ_L, according to the arguments given earlier, we refer to the electron thermal energy balance equation which we write as

$$E_{\parallel} J_{\parallel} = \nu_E^{e,i}\, nT_e + \nu_E\, nT_e \qquad (7.4)$$

where $\nu_E^{e,i}$ represents the rate of energy transfer to to the ions and ν_E the rate of direct energy loss by conduction, radiation, etc. Then we have, for $u_e/v_{the} \approx \xi_L$ and $\alpha_E \approx \xi_L/2A_T$

$$\frac{2}{A_T}\,\xi_L^2 = \frac{\nu_E^{e,i}}{\nu_{ei}} + \frac{\nu_E}{\nu_{ei}} \qquad (7.5)$$

If $\nu_E^{e,i}$ is only given by electron-ion collisions, $\nu_E^{ei} = (3m_e/m_i)(1 - T_i/T_e)\nu_{ei}$ and

$$\xi_L = A_T^{1/2} \left(\frac{3}{2}\,\frac{m_e}{m_i}\right)^{1/2} \left[1 - \frac{T_i}{T_e} + \frac{2}{3}\,\frac{m_i}{m_e}\,\frac{\nu_E}{\nu_{ei}}\right]^{1/2} \qquad (7.6)$$

In the case of H_2 plasmas, $[3m_e/(2m_i)]^{1/2} \approx 0.03$, and this may be a good estimate of the observed beginning of regime II to the extent that the quantity multiplying this factor in Eq.(7.6) is of order unity.

When increasing ξ towards ξ_C, the positive slope of f_e that tends to develop for $v_{\parallel} \geq (2r/R_0)^{1/2}\, v_{the}$ leads to the excitation of modes that prevent the circulating electron distribution from separating from the one of trapped electrons. Then the type of distribution that is observed should depend on the distance Δr of the point of observation from the magnetic axis which, in turns, depends on factors such as the values of the externally applied vertical and horizontal magnetic fields, the metallic shell surrounding the plasma column, and the plasma pressure. In particular, we notice that even if Δr is relatively small, the fraction of trapped electrons can be appreciable. For instance, if Δr = 1 cm, this fraction is about 20%.

iii) EMISSION AT THE "REDUCED" PLASMA FREQUENCY

We recall that the electron Langmuir frequency is numerically

$$\omega_{pe} \approx 28.3 \times \hat{n}^{1/2}\ \text{GHz}$$

where $\hat{n} = n/(10^{13}\ \text{cm}^{-3})$. Thus the possible modes that can be excited at the reduced plasma frequency $(k_{\parallel}\omega_{pe}/k)$ have

$$\omega \geq \frac{a}{R_0 q_0}\,\omega_{pe} = \left(\frac{a}{9}\right)\left(\frac{3}{q_0}\right)\left(\frac{54}{R_0}\right) \times \hat{n}^{1/2} \times 1.6\ \text{GHz}$$

Since the density range over which the "slide-away" regime is produced in Alcator is $0.5 \leq \hat{n} \leq 2$, it is natural to associate the emission detected for $\omega > 1$ GHz with this kind of mode. The emission at these frequencies that accompanies the ω_{pi} mode can be explained in terms of the higher branch of the dispersion relation represented by Fig.8.

Another possibility is provided by the instability discussed at the end of Section 4. In this connection, we may consider the case where the second of the two relevant resonances

$$\Omega_e = k_{\parallel} v_{\parallel} \quad \text{and} \quad \omega_{pe} = k\, v_{\parallel}$$

involves a region where, before the onset of the slide-away regime when the ω_{pi} mode is not yet excited, the slope of the electron distribution is sufficiently small that the destabilizing effect associated with the first resonance prevails. In reference to the same form of emission as we have described in sub-section (i), it may also be possible that, as a result of collisions as well as of collective modes, a considerable part of the electron distribution remains tied to the trapped portion of it. Therefore, only a small fraction, in the distribution tail, is allowed to run away as a whole and set up a configuration of the type indicated in Fig.13, which can drive the considered mode unstable. A possible means to "freeze" the electron distribution into the configuration indicated by Fig.13 can be provided by the excitation of a standing mode of the type considered in Section 6, which extracts energy from the region where the electron distribution has positive slope and transfers it to the region with opposite values of $v_{\parallel}$, while momentum is exchanged with the magnetic field.

ACKNOWLEDGEMENTS

It is a pleasure to thank the members of the Alcator team and, in particular, R. Parker and R. Taylor for a fruitful and continuing interaction and G. Lampis for all his collaboration. This work was supported in part by the Energy Research and Development Administration, Contract EA(11-1) 3070.

APPENDIX

RELATIVISTIC CORRECTIONS TO THE CYCLOTRON RESONANCE CONDITION

We shall write the wave-particle resonance condition using a quantum-mechanical picture. From the relativistic (spinless) Hamiltonian of an

electron in a constant and uniform magnetic field described by the vector potential $\vec{A} = -B_z y \vec{e}_x$

$$\mathcal{H} = \left[m_0^2 c^4 + c^2 \left(\vec{p} - \frac{e}{c} \vec{A} \right)^2 \right]^{1/2} \qquad (A.1)$$

we derive the Klein-Gordon equation

$$\frac{1}{c^2} \frac{\partial^2 \psi}{\partial t^2} - \frac{\partial^2 \psi}{\partial z^2} - \frac{\partial^2 \psi}{\partial y^2} + (y - y_0)^2 \frac{e^2 B^2}{\hbar^2 c^2} \psi + \frac{m_0^2 c^2}{\hbar^2} \psi = 0 \qquad (A.2)$$

where ψ is the spinless electron wave function and y_0 is the classical y-co-ordinate of the centre of gyration. Solving Eq.(A.2), we find the spectrum of the Hamiltonian (A.1) [33]

$$E = (m_0^2 c^4 + p_z^2 c^2 + (2n+1) m_0 c^2 \hbar |\Omega_e|)^{1/2} \qquad (A.3)$$

where $\Omega_e = -eB/m_0 c$ is the non-relativistic cyclotron frequency, and n = 0, 1, ... is the quantum number of the Landau levels.

The energy-momentum conservation equations describing the absorption of a wave-quantum by an electron are

$$\hbar\omega = \Delta E, \qquad \hbar k_\parallel = \Delta p_z \qquad (A.4)$$

From Eq.(A.3) we have

$$\Delta E = c^2 \frac{p_z \Delta p_z}{E} + E(p_z, n + \Delta n) - E(p_z, n) \qquad (A.5)$$

We are interested in the limit in which $m_0^2 c^2 \gtrsim p_z^2$ and $m_0 c^2 \gg (2n+1)\hbar |\Omega_e|$ so that

$$\Delta E \simeq \frac{c^2 p_z \Delta p_z}{(m_0^2 c^4 + c^2 p_z^2)^{1/2}} + \frac{m_0 c^2 \hbar |\Omega_e|}{(m_0^2 c^4 + p_z^2 c^2)^{1/2}} \Delta n = v_\parallel \Delta p_z + \hbar |\Omega_e| \gamma^{-1} \Delta n \qquad (A.6)$$

where $\gamma = (1 - v_\parallel^2/c^2)^{-1/2}$. For the case $\Delta n = 1$, neglecting ω compared to $|\Omega_e|\gamma^{-1}$ (namely, assuming $\Delta E \simeq 0$), from Eqs (A.4) and (A.6) we obtain the resonance condition:

$$\gamma k_\parallel v_\parallel = \Omega_e \qquad (A.7)$$

REFERENCES

[1] SPITZER, L., HÄRM, R., Phys. Rev. 89 (1953) 977.
[2] COPPI, B., POZZOLI, R., Plasma Phys. 16 (1974) 223.
[3] COPPI, B., REWOLDT, G., in Advances in Plasma Physics, (SIMON, A., THOMPSON, W.B., Eds) 6, Interscience, New York (1976) 421.
[4] COPPI, B., LAVAL, G., PELLAT, R., ROSENBLUTH, M.N., Nucl. Fusion 6 (1968) 261.
[5] COPPI, B., Rivista Nuovo Cim. 1 (1969) 357.
[6] COPPI, B., OOMENS, A., PARKER, R., PIERONI, L., SCHULLER, F., SEGRE, S., TAYLOR, R., M.I.T. Report PRR-7417, Cambridge, Massachusetts (1974).
[7] COSTLEY, A.E., HASTIE, R.J., PAUL, J.W.M., CHAMBERLAIN, J., Phys. Rev. Lett. 33 (1974) 758.
[8] COPPI, B., PEGORARO, F., POZZOLI, R., REWOLDT, G., M.I.T. Report PRR-758, Cambridge, Massachusetts (1975).
[9] COPPI, B., POZZOLI, R., REWOLDT, G., SCHEP, T., in Plasma Physics and Controlled Nuclear Fusion Research (Proc. 5th Int. Conf. Tokyo, 1974) 1, IAEA, Vienna (1975) 549.
[10] BOXMAN, G.J., COPPI, B., DeKOCK, L.C.J.M., MEDDENS, B.J.H., OOMENS, A.A., ORNSTEIN, L.T.M., PAPPAS, D.S., PARKER, R.R., PIERONI, L., SEGRE, S.E., SCHUELLER, F.C., TAYLOR, R.J., Invited paper at the VIIth European Conference on Plasma Physics, Lausanne, Switzerland (1975). Proceedings to be published by the European Physical Society.
[11] ROSENBLUTH, M.N., HAZELTINE, R.D., HINTON, F.L., Phys. Fluids 15 (1972) 116.
[12] COPPI, B., REM, J., Phys. Fluids 17 (1974) 184.
[13] COPPI, B., ROSENBLUTH, M.N., SUDAN, R.N., Ann. Phys. 55 (1969) 207.
[14] CORDEY, J.G., HOUGHTON, M.J., Nucl. Fusion 13 (1973) 215, in which a similar dispersion relation is derived for the case of an injected neutral beam.
[15] BUSSAC, M.N., LAVAL, G., PELLAT, R., Phys. Rev. Lett. 30 (1973) 588.
[16] KENNEL, C.F., ENGELEMANN, F., Phys. Fluids 9 (1966) 2377.
[17] COPPI, B., MAZZUCATO, E., Phys. Fluids 14 (1971) 134.
[18] COPPI, B., LAMPIS, G., PEGORARO, F., PIERONI, L., SEGRE, S., M.I.T. Report PRR 7521, Cambridge, Massachusetts (1975). To be published.
[19] KADOMTSEV, B.B., POGUTSE, O.P., Sov. Phys. - JETP 26 (1968) 1146.
[20] COPPI, B., KULSRUD, R., OBERMAN, C., private communication (1969).
[21] COPPI, B., TARONI, A., Plasma Phys. 16 (1974) 161.
[22] ROSENBLUTH, M.N., in Plasma Physics, IAEA, Vienna (1965) 485.
[23] COPPI, B., Lett. Nuovo Cim. 10 (1974) 156.
[24] HIROSE, A., MAH, S.Q., SKARSGARD, H.M., STRILCHUK, A.R., WHITFIELD, D.W.A., Phys. Rev. Lett. 28 (1972) 1185.
[25] PIERONI, L., SEGRE, S.E., Phys. Lett. 51A (1975) 25.
[26] PIERONI, L., SEGRE, S.E., Phys. Rev. Lett. 34 (1975) 928.
[27] LAMPIS, G., private communication (1975).
[28] KOMM, D., private communication.
[29] COPPI, B., DOBROWOLNY, M., SANTINI, F., M.I.T. Report PRR-724, Cambridge, Massachusetts (1972).
[30] DREICER, H., Phys. Rev. 115 (1959) 238.
[31] KULSRUD, R.M., SUN, Y.C., WINSOR, N.S., FALLON, H.A., Phys. Rev. Lett. 31 (1973) 690.
[32] BRAGINSKII, S.I., in Reviews of Plasma Physics. (LEONTOVICH, M.A., Ed.) 1, Consultants Bureau, New York (1965) 205.
[33] RABI, I.I., Z. Physik 49 (1928) 7. Here the spectrum is properly derived by using the Dirac equation, which replaces the factor (2n+1) in Eq.(A.3) by (2n), due to spin corrections.

(Manuscript received 25 August 1975
Final version received 28 January 1976)